

Clusters and Groups of Galaxies in the Simulated Local Universe

Luca Casagrande^{1,2*} and Antonaldo Diaferio³

¹ *Tuorla Astronomical Observatory, Piikkiö, Finland*

² *University of Turku, Finland*

³ *Dipartimento di Fisica Generale “Amedeo Avogadro”, Università degli Studi di Torino, Italy*

10 November 2018

ABSTRACT

We compare the properties of galaxy groups extracted from the Updated Zwicky Catalogue (UZC) with those of groups extracted from N -body simulations of the local Universe, in a Λ CDM and a τ CDM cosmology. In the simulations, the initial conditions of the dark matter density field are set to reproduce the present time distribution of the galaxies within $80h^{-1}$ Mpc from the Milky Way. These initial conditions minimize the uncertainty originated by cosmic variance, which has affected previous analyses of this small volume of the Universe. The simulations also model the evolution of the photometric properties of the galaxy population with semi-analytic prescriptions. The models yield a galaxy luminosity function sensibly different from that of the UZC and are unable to reproduce the distribution of groups and their luminosity content. The discrepancy between the model and the UZC reduces substantially, if we redistribute the luminosity among the galaxies in the simulation according to the UZC luminosity function while preserving the galaxy luminosity rank. The modified Λ CDM model provides the best match to the UZC: the abundances of groups by harmonic radius, velocity dispersion, mass and luminosity are consistent with observations. We find that this model also reproduces the halo occupation number of groups and clusters. However, the large-scale distribution of groups is marginally consistent with the UZC and the redshift-space correlation function of galaxies on scales larger than $6h^{-1}$ Mpc is still more than $3\text{-}\sigma$ smaller than observed. We conclude that reproducing the properties of the observed groups certainly requires a more sophisticated treatment of galaxy formation, and possibly an improvement of the dark matter model.

Key words: methods: miscellaneous – galaxies: clusters: general – galaxies: formation – cosmology: miscellaneous – dark matter – large-scale structure of Universe.

1 INTRODUCTION

The formation and evolution of galaxies is one of the major challenges of cosmology. Within the framework of the hierarchical structure formation by gravitational instability, galaxies properties are strongly affected by their environment. Most galaxies reside in groups and much work on compact (Hickson 1997 and references therein; Barton et al. 2003; Mendes de Oliveira et al. 2003; Lee et al. 2004; Kelm & Focardi 2004; Tovmassian, Plionis & Torres-Papaqui 2006) and loose groups (Postman & Geller 1984; Allington-Smith et al. 1993; Tran et al. 2001; Martínez et al. 2002a,b; Tanvuia et al. 2003; Girardi et al. 2003; Balogh et al. 2004;

Weinmann et al. 2006a; Zandivarez, Martínez & Merchán 2006; Martínez & Muriel 2006; Brough et al. 2006) shows that these systems can be more effective than clusters at shaping the properties of galaxies, namely morphology, luminosity, color, star formation rate and cold gas content (see also Kodama et al. 2001; Ellingson 2004; Verheijen 2004; Tanaka et al. 2005).

Galaxy groups trace the large-scale distribution of galaxies (e.g. Berlind et al. 2006), and thus describe the distribution of the optical light from sub-megaparsec scales to the largest scale probed. Models of galaxy formation should be able to reproduce the properties of galaxy groups. For an appropriate comparison of models with observations, however, the surveyed volume of the real groups must be sufficiently large to be representative of the Universe. Over the last years, the compilation of deep galaxy redshift surveys

* E-mail: luccas@utu.fi (LC), diaferio@ph.unito.it (AD)

has provided galaxy group catalogues with an increasing number of systems (Ramella et al. 1999; Eke et al. 2004a; Berlind et al. 2006 and references therein). These catalogues are deep enough to average out the large-scale structure fluctuations and obtain a robust estimate of the light distribution.

In current models, large-scale structure forms by the gravitational collapse of dark matter, which dominates the dynamics of galaxy systems. Comparing models with data therefore requires a valuable treatment of the dynamics of the baryonic matter within the dark matter halos. Diaferio et al. (1999) were the first to attempt to compare real redshift surveys with mock surveys where galaxies were formed and evolved with semi-analytic prescriptions applied to merger trees of dark matter halos extracted from N -body simulations. They compared the model with the northern sector of the Updated Zwicky Catalog (UZC) redshift survey (Falco et al. 1999). This comparison resulted in a general agreement between the now standard Cold Dark Matter model with a non-zero cosmological constant (Λ CDM) and observations, although the mean luminosity of the simulated groups was smaller than observed. A further topological analysis of the mock redshift surveys and the UZC quantified how the large-scale structure was much fuzzier in the mock catalogues than in the UZC (Schmalzing & Diaferio 2000). Both disagreements were tentatively attributed to cosmic variance, responsible for the lack, in the mock surveys, of a coherent structure as thin and wide as the Great Wall. The UZC is only $150h^{-1}$ Mpc deep and indeed its volume is not large enough to suppress the fluctuations of the large-scale structure. Therefore a fair comparison of the model with the UZC requires a not-random choice of the volume in the simulations.

Mathis et al. (2002) perform N -body simulations where the initial conditions are constrained to reproduce the large-scale distribution of galaxies observed in the IRAS 1.2 Jy survey (Fisher et al. 1995) within $80h^{-1}$ Mpc of the Milky Way. In their simulations, Mathis et al. (2002) also include semi-analytic recipes to form and evolve galaxies. Thus, these simulations seem appropriate to test whether the current galaxy formation models yield the observed clustering and luminosity properties of groups once the large scale distribution of galaxies faithfully mirror the real one. This paper is devoted to this test.

Sect. 2 summarizes the properties of the constrained simulations; sects. 3 and 4 describe our real and mock galaxy redshift surveys and our group catalogues in redshift space. In sect. 5 we investigate the large-scale distribution of groups and in sect. 6 we discuss the distribution of light among and within groups. We conclude in sect. 7.

2 THE SIMULATION OF THE LOCAL UNIVERSE

The constrained simulations we use here combine the N -body technique with the semi-analytic approach for the formation of galaxies to predict the evolution of both the photometric properties of galaxies and their phase space coordinates, following a strategy pioneered by Roukema et al. (1997) and Kauffmann et al. (1999).

The simulations were run by Mathis et al. (2002) who

provide extensive details in their original paper. They investigate two variants of a flat cold dark matter (CDM) universe: a Λ CDM model, with cosmological density parameter $\Omega_0 = 0.3$, cosmological constant $\Lambda = 0.7$, and Hubble constant $H_0 = 70 \text{ km s}^{-1}\text{Mpc}^{-1}$, and a τ CDM model, with $\Omega_0 = 1$ and $H_0 = 50 \text{ km s}^{-1}\text{Mpc}^{-1}$. For both models, the normalization of the power spectrum of the initial density perturbations is imposed by the abundance of galaxy clusters at the present time: $\sigma_8 = 0.9$ and 0.6 for the Λ CDM and τ CDM models, respectively.

The initial conditions at $z = 50$ are set to reproduce the observed present-day galaxy density field, provided by the IRAS 1.2 Jy survey (Fisher et al. 1994; 1995), within a sphere of radius $80 h^{-1}$ Mpc centered on the Milky Way and smoothed with a Gaussian filter with one-dimensional dispersion $5 h^{-1}$ Mpc. The constrained initial displacement field for the dark matter particles for all wavenumbers in the range $k_0 = 2\pi/L$ and $64k_0$, on a simulation cube of side $L = 240h^{-1}$ Mpc, is generated with the Hoffman-Ribak algorithm (Hoffman & Ribak 1991, 1992; Ganon & Hoffman 1993). The high-frequency field in the wavenumber range $64k_0 - 343k_0$ is unconstrained. Therefore, the distribution of matter on scales smaller than $5 h^{-1}$ Mpc is unrelated to the real Universe. The simulation contains two populations of particles: the high-resolution particles, which will end up within $80 h^{-1}$ Mpc from the center of the simulation box (the location of the Milky Way) by $z = 0$, and more massive low-resolution particles, which will remain outside this region. The simulation box contains $\sim 5 \times 10^7$ high-resolution particles with individual mass $0.36 \times 10^{10} h^{-1} M_\odot$ and $1.2 \times 10^{10} h^{-1} M_\odot$ in the Λ CDM and τ CDM model, respectively.

The equations of motion of the dark matter particles are integrated with the tree-code GADGET (Springel, Yoshida & White 2001). The halo merger trees are then extracted from the simulation and provided as input to the semi-analytic code used to form and evolve galaxies within the dark matter halos. Apart from a few differences, Mathis et al. (2002) use the same recipes that Kauffmann et al. (1999) applied to the GIF simulations. The simulations have enough mass and spatial resolution to follow the formation of all galaxies brighter than the Large Magellanic Cloud that will end up, by $z = 0$, within the nearly spherical high-resolution region of radius $80 h^{-1}$ Mpc centered on the Milky Way. The luminosity resolution of the simulations are $M_B = -15.48 + 5 \log h$ and $-16.94 + 5 \log h$ for the Λ CDM and τ CDM models, respectively. Note that the limits mentioned in Mathis et al. (2002) differ from those provided on their web site. Here we adopt the latter. To these limits, the Λ CDM and τ CDM models contain 189122 and 194243 galaxies in the high-resolution volume.

3 MOCK AND REAL REDSHIFT SURVEYS

We extract mock redshift surveys from the simulations to perform a detailed comparison with the UZC (Falco et al. 1999). This catalogue is currently the magnitude-limited redshift survey of the local universe with the widest sky coverage in the optical band. The UZC has been extensively investigated: Schmalzing & Diaferio (2000) analyze its topology, Padmanabhan, Tegmark & Hamilton (2001) com-

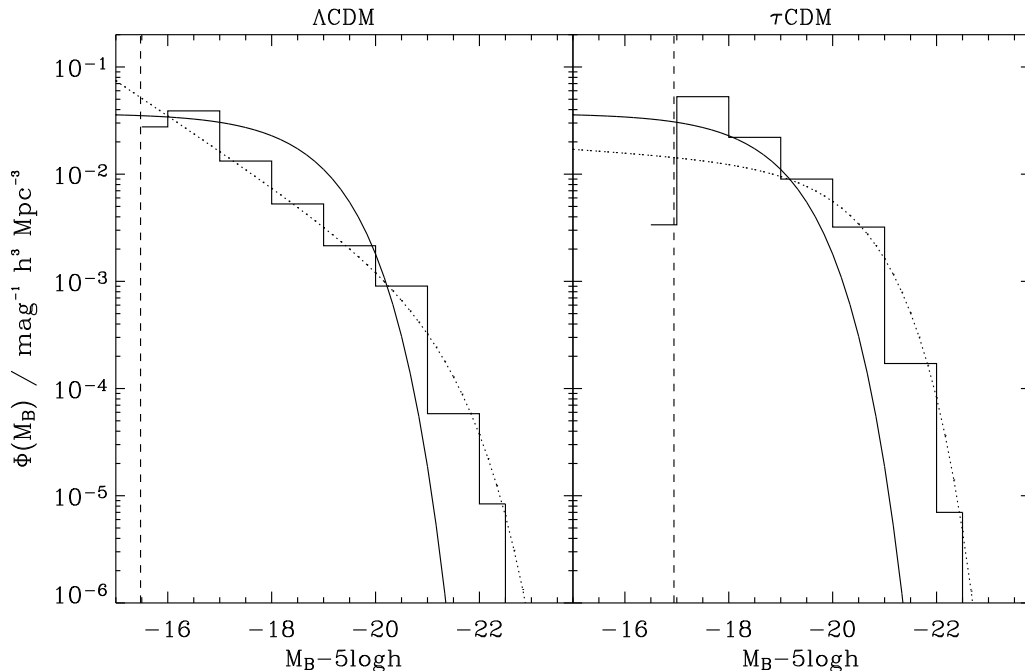


Figure 1. The B -band luminosity functions in the simulations. The vertical lines show the luminosity resolution. The dotted lines are the fits to the Schechter function (Table 1). The solid lines are the M_{Zw} -band luminosity function of the UZC (Marzke, Huchra & Geller 1994).

pute its redshift space power spectrum, Hoyle & Vogeley (2002) investigate the void properties, and much work is dedicated to galaxy groups and pairs (Padilla et al. 2001; Ramella et al. 2002; Focardi & Kelm 2002; Pisani et al. 2003; Plionis et al. 2004; Ceccarelli et al. 2005; Berrier et al. 2006; Focardi et al. 2006). Moreover, Diaferio et al. (1999) performed a detailed comparison of the GIF simulations (Kauffmann et al. 1999) with the CfA2N, the subsample of the UZC galaxies in the northern galactic hemisphere.

Here, we consider the region limited by $-2.5^\circ \leq \delta_{1950} \leq 50^\circ$ and $8^h \leq \alpha_{1950} \leq 17^h$ in the North Galactic Cap (hereafter NGC) and by $20^h \leq \alpha_{1950} \leq 4^h$ in the South Galactic Cap (hereafter SGC). This survey region is 98 per cent complete down to the Zwicky magnitude $m_{Zw} = 15.5$ (Falco et al. 1999). We also apply a Galactic cut $-13^\circ \leq b \leq 13^\circ$ and further discard the southern Galactic region with $\alpha_{1950} \geq 3^h$ to reduce extinction problems (Padmanabhan et al. 2001; Ramella et al. 2002). Finally, we only consider galaxies with redshift $cz < 8000 \text{ km s}^{-1}$, because the simulated high-resolution region is limited to $80h^{-1} \text{ Mpc}$ from the Milky Way. The redshift surveys we extract cover roughly a quarter of the sky and contain more than 7000 galaxies.

To extract mock redshift surveys from the simulation box, we place an observer at the center of the box where the Milky Way is located and assign celestial coordinates to the simulated galaxies. Each galaxy in the simulations has radial velocity $cz = \mathbf{v} \cdot \mathbf{r} / \|\mathbf{r}\| + \|\mathbf{r}\|$, where \mathbf{v} is the galaxy peculiar velocity and \mathbf{r} is the galaxy position vector, in units of km s^{-1} . Further details on the construction of the samples are given below.

Table 1. Luminosity function parameters. For the UZC M^* is in the Zwicky system.

	α	$M_B^* - 5 \log h$	$\phi^* / h^3 \text{Mpc}^{-3} \text{mag}^{-1}$
UZC	-1.00	-18.80	4.00×10^{-2}
Λ CDM	-1.82	-21.08	8.39×10^{-4}
τ CDM	-1.08	-20.29	1.28×10^{-2}

3.1 The SALF catalogues

3.1.1 Mock catalogues

The UZC is magnitude limited to the Zwicky magnitude $m_{Zw} = 15.5$, whereas the mock catalogues contain galaxies with B -band apparent magnitudes $m_B = M_B + 25 + 5 \log(r/h^{-1} \text{Mpc})$. Therefore, we need to transform the Zwicky magnitude limit into the simulated B -band. Detailed calibrations of observed samples seem to imply $m_{Zw} \sim m_B$, but with a rather large $1\text{-}\sigma$ scatter of $\sim 0.3 \text{ mag}$ (Huchra 1976; Bothun & Cornell 1990; Marzke, Huchra & Geller 1994). Moreover the luminosity functions of the galaxies in the simulations and in the UZC are sensibly different, as we discuss below, and assuming naively $m_{Zw} = m_B$ would not provide reliable results. Therefore, following Diaferio et al. (1999) and Mathis et al. (2002), we adjust the magnitude cut-off of the simulated surveys to obtain a number of galaxies in the mock surveys comparable to the number in the UZC.

This constraint imposes the magnitude limits

- (i) $m_B = m_{Zw} + 0.7 = 16.2$ in NGC
- (ii) $m_B = m_{Zw} + 0.4 = 15.9$ in SGC

for the the Λ CDM model, and

- (i) $m_B = m_{Zw} - 0.6 = 14.9$ in NGC
- (ii) $m_B = m_{Zw} - 0.9 = 14.6$ in SGC

for the τ CDM model. Unlike Mathis et al. (2002), we therefore use different transformations for NGC and SGC. These different limits are consistent with the 0.3 mag scatter mentioned above and could be due to differences in the photometric zero-point across the different regions of the sky. A few of the many claimed systematic errors in the Zwicky catalogue are supported by clean observational evidence and a unique interpretation of this discrepancy between NGC and SGC is still lacking (Marzke, Huchra & Geller 1994). We note that the transformations for NGC are similar to those adopted by Diaferio et al. (1999) in the GIF simulations which contained semi-analytic prescriptions similar to those of Mathis et al. (2002). In the UZC and mock catalogues we also exclude galaxies with redshift $cz < 500$ km s⁻¹ and $m_{Zw} < 10$ to avoid bright objects close to the Milky Way.

3.1.2 The UZC

In order to make a proper comparison with the simulations, in the UZC we have to exclude galaxies that are fainter than the luminosity resolution of the corresponding simulation. This is especially important for NGC, where the nearby Virgo cluster has many faint galaxies that cannot be resolved by the simulations.

Therefore we compile two UZC catalogues, one where we exclude all galaxies fainter than the Λ CDM luminosity resolution ($M_B = -15.48 + 5 \log h$: UZC- Λ -SALF) and another where we exclude all galaxies fainter than the τ CDM luminosity resolution ($M_B = -16.94 + 5 \log h$: UZC- τ -SALF).

In principle, the luminosity resolution cut should be done in the Zwicky and not in the B -band magnitude. As we have discussed above, the transformation between the two systems is uncertain and possible differences in the zero-points of NGC and SGC make the transformation more complicated, because different cuts would be required for different regions of the sky. Fortunately, the luminosity resolution cut only concerns the nearby and faintest galaxies and a change of ± 0.3 mag in the luminosity resolution limit reflects into a difference of ± 170 galaxies, at most, in the final UZC number of galaxies. Furthermore, in the UZC the luminosity resolution cut applies in redshift space, whereas the luminosity resolution limit of the simulation is in real space. When building mock redshift surveys, the effect of peculiar velocities blurs such a limit. Given such uncertainties, it is reasonable to use the simulated B -band limits to cut the UZC galaxies in the Zwicky magnitude.

3.2 The UZCLF catalogues

The properties of the galaxy distribution in a magnitude-limited redshift survey depend both on the distribution of galaxies in real space and on their luminosity function. Figure 1 shows the galaxy luminosity function in the two simulations, with their best fits to a Schechter function (Table 1). The model functions are sensibly different from the luminosity function of the UZC derived by Marzke et al. (1994). In order to separate the role of the large-scale distribution

of galaxies from their luminosity function in our comparison between the models and the UZC, we replace the luminosities of galaxies predicted by the semi-analytic procedure with luminosities extracted from the UZC luminosity function (Marzke et al. 1994).

For each model we find the new luminosity resolution limit L_{lim} which satisfies the relation

$$V \int_{L_{lim}}^{\infty} \phi_{UZC}(L) dL = N \quad (1)$$

where $\phi_{UZC}(L)$ is the UZC luminosity function (see Table 1), N is the number of simulated galaxies more luminous than the semi-analytical luminosity resolution and V is the high-resolution volume of the simulation box. We then randomly sample N luminosities in the range $[L_{lim}, +\infty]$ which distribute accordingly to $\phi_{UZC}(L)$ and assign these new luminosities to the simulated galaxies while preserving the luminosity rank predicted by the semi-analytic prescriptions. The new luminosity resolutions L_{lim} are $M_{Zw} = -15.85 + 5 \log h$ and $M_{Zw} = -15.78 + 5 \log h$ for the Λ CDM and τ CDM models, respectively. The luminosity function of the simulated galaxies now perfectly matches $\phi_{UZC}(L)$ and the only galaxy property imposed by the model is the galaxy luminosity rank.

Even if the luminosities are now constrained to match the UZC luminosity function, a magnitude limit $m_{lim} = 15.5$ for the mock catalogues does not necessarily return the same number of galaxies as observed. In fact, both the aforementioned uncertainties in the Zwicky magnitudes and the large-scale distribution of galaxies in the small UZC volume can affect the galaxy number of a magnitude-limited survey. Even if the simulations we use are intended to minimize the cosmic variance uncertainty by reproducing the gross features of the large-scale structure, the total number N of the simulated galaxies still depend on the semi-analytic prescriptions. Therefore, we adopt the following limiting magnitudes for the mock catalogues, in order to recover a number of galaxies approximately equal to that of the UZC :

- (i) $m_{lim} = 15.3$ in NGC
- (ii) $m_{lim} = 15.0$ in SGC

for the the Λ CDM model, and

- (i) $m_{lim} = 15.5$ in NGC
- (ii) $m_{lim} = 15.1$ in SGC

for the τ CDM model. As for the SALF catalogues, the difference between NGC and SGC is ~ 0.3 mag. All the apparent magnitudes of the galaxies are then increased by the difference between the appropriate m_{lim} and 15.5 in order to have the same zero-point of the photometric system in NGC and SGC. We now have mock catalogues with the same number of galaxies and the same luminosity function as the UZC, but with the large-scale structure and the velocity field predicted by the underlying cosmological model.

As for the SALF catalogues, we also make different catalogues from the real UZC, where we exclude all galaxies fainter than the appropriate luminosity resolutions: we thus have a UZC- Λ -UZCLF and a UZC- τ -UZCLF catalogue.

Table 2 lists the number of galaxies in each catalogue. Figures 2 – 5 show the UZC and the mock redshift surveys.

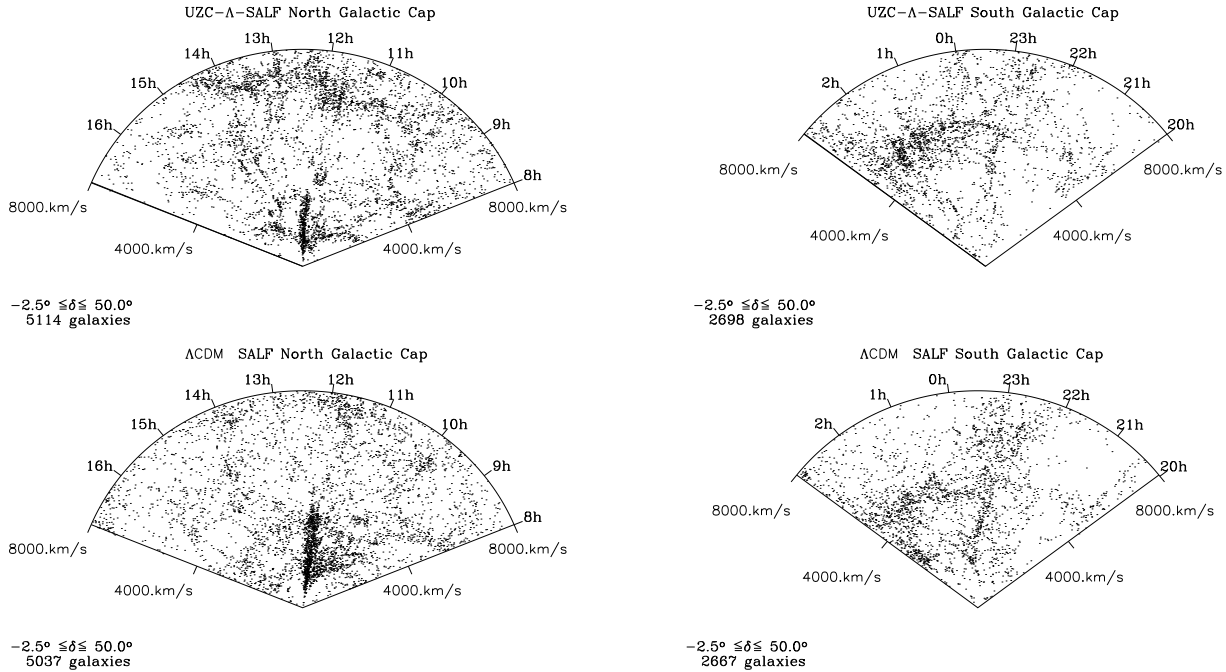


Figure 2. The distribution of the galaxies (dots) in the magnitude-limited UZC-A-SALF and in the mock ACDM-SALF redshift surveys.

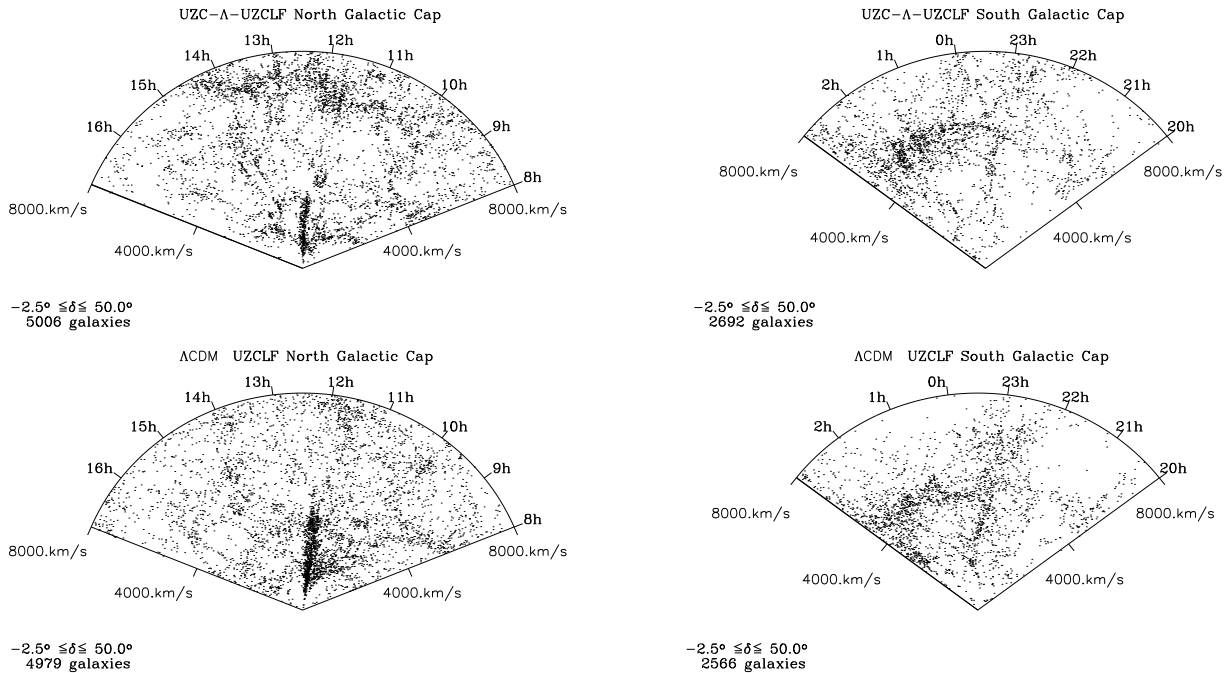


Figure 3. The distribution of the galaxies (dots) in the magnitude-limited UZC-A-UZCLF and in the mock ACDM-UZCLF redshift surveys.

4 THE GROUP IDENTIFICATION

We identify groups in redshift space in the UZC and in our mock catalogues with the friends-of-friends (FOF) algorithm described in Ramella, Pisani & Geller (1997). We use the linking parameter $V_0 = 350 \text{ km s}^{-1}$ and the number density contrast $\delta n/n = 80$ at the fiducial velocity $V_F = 1000 \text{ km s}^{-1}$. These parameters minimize the fraction

of interlopers and provide the best estimates of the properties of groups identified in real space (Diaferio et al. 1999). Nevertheless, these linking parameters still yield group catalogues where ~ 40 per cent of the triplets and ~ 20 per cent of the groups with four or more members are accidental superpositions of galaxies (spurious groups). Therefore, following Mahdavi et al. (2000) and Ramella et al. (2002), we restrict our catalogues to groups with $N \geq 5$ members

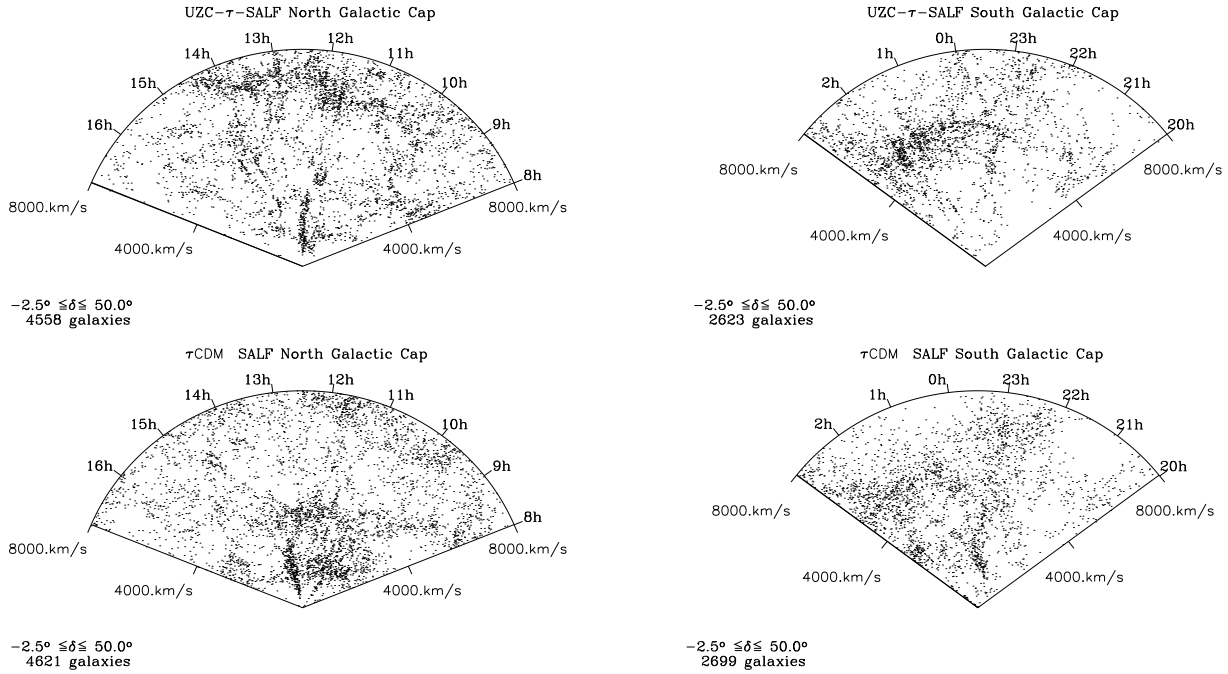


Figure 4. The distribution of the galaxies (dots) in the magnitude-limited UZC- τ -SALF and in the mock τ CDM-SALF redshift surveys.

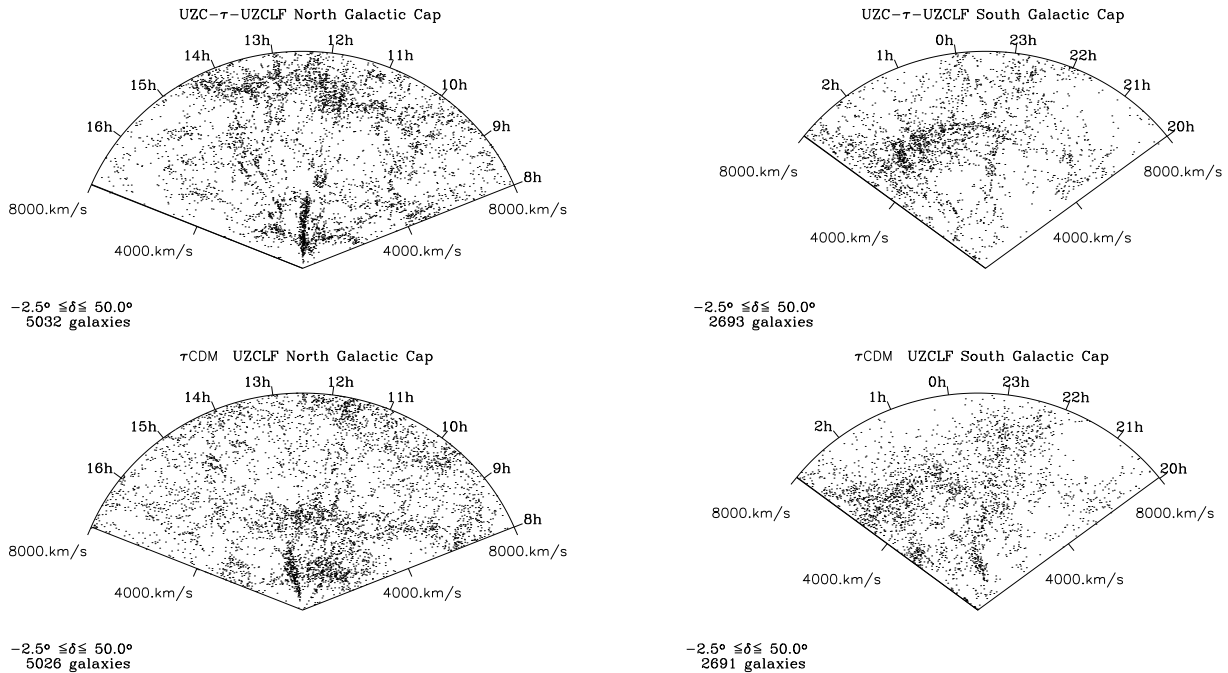


Figure 5. The distribution of the galaxies (dots) in the magnitude-limited UZC- τ -UZCLF and in the mock τ CDM-UZCLF redshift surveys.

when we derive the physical properties of groups. However, to limit the shot-noise, we include all groups with $N \geq 3$ members when we compute the two-point correlation function of groups.

We consider groups with mean velocities in the range $500 < cz < 7000 \text{ km s}^{-1}$. The lower limit avoids groups close to the Milky Way and the upper limit excludes groups which are too close to the edge of the mock survey. Figures

6–9 show the location of the groups in the UZC and in the model surveys.

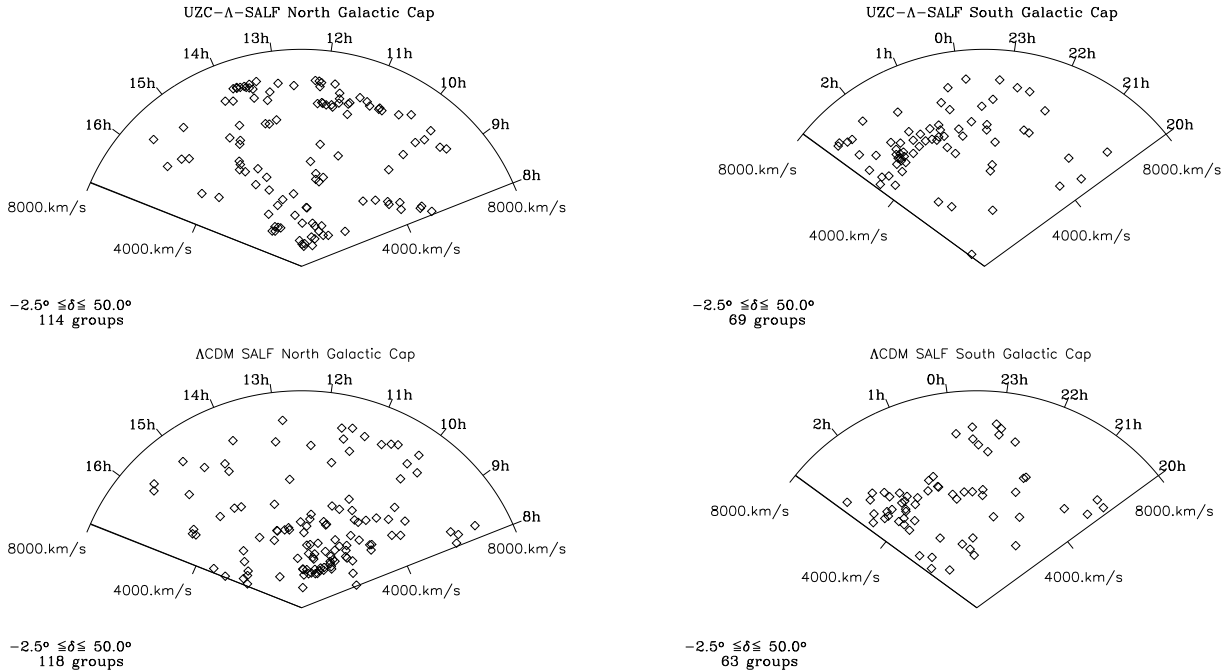


Figure 6. The distribution of groups (diamonds) in the UZC-A-SALF and in the mock ACDM-SALF redshift surveys.

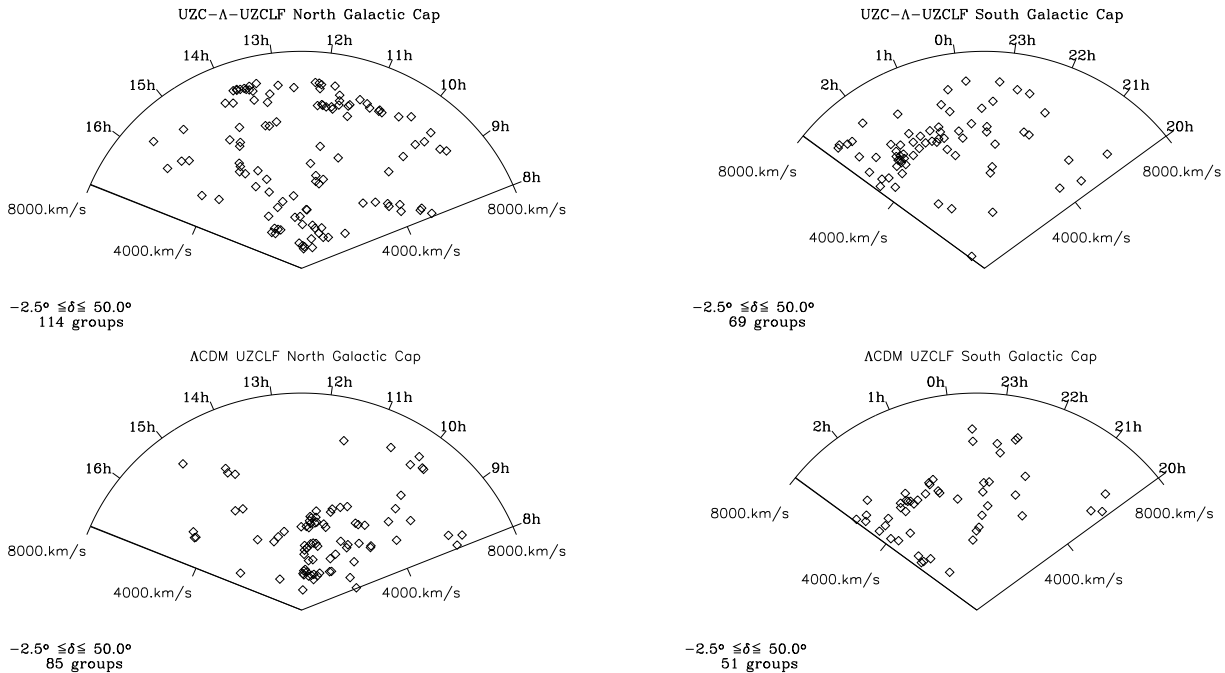


Figure 7. The distribution of groups (diamonds) in the UZC-A-UZCLF and in the mock ACDM-UZCLF redshift surveys.

5 GROUPS AS TRACERS OF THE LARGE-SCALE STRUCTURE

Figures 2 – 5 show that both the Λ CDM and the τ CDM models reproduce the gross features of the local Universe, as imposed by the initial conditions. However, neither model has structures as sharply defined as in the real Universe. In particular, the τ CDM model has much looser structures

than the Λ CDM model and the UZC, and this reflects into much lower fractions of galaxies in groups (see Table 3).

Schmalzing & Diaferio (2000) quantified this disagreement in mock redshift surveys extracted from the GIF simulations. They used the Minkowski functionals to show that the UZC has a substantially larger degree of planarity than the models. They concluded that cosmic variance can be responsible for the inability of the models at reproducing large two-dimensional structures like the Great Wall, which

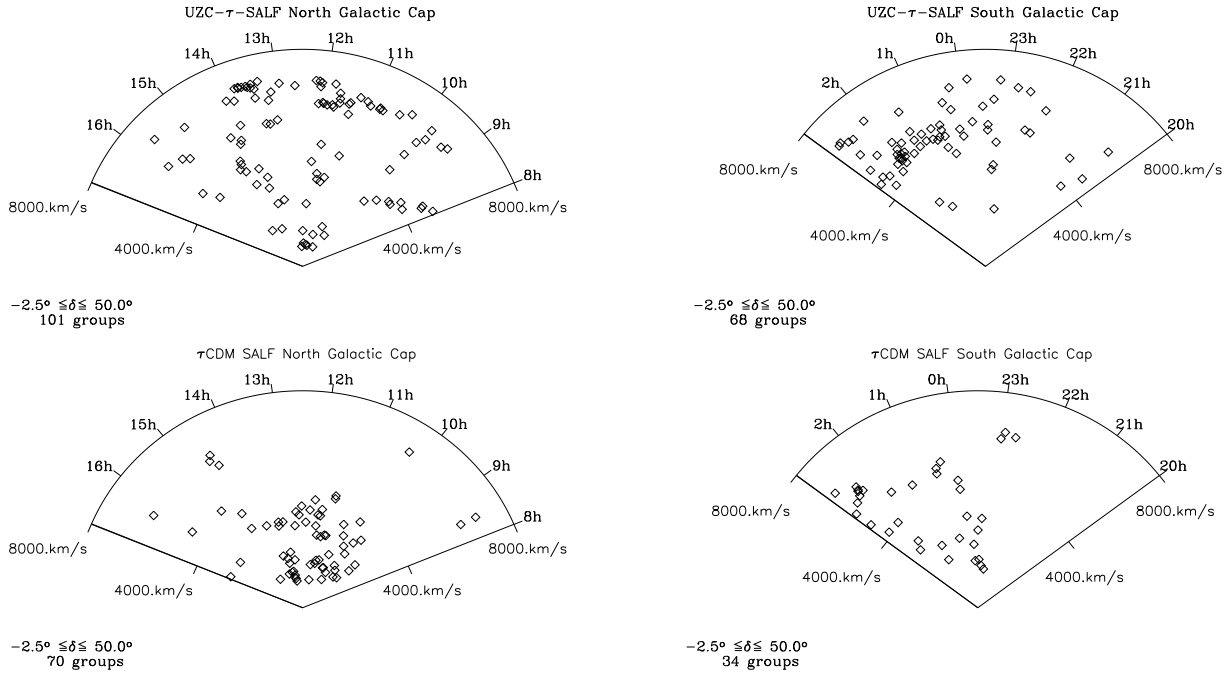


Figure 8. The distribution of groups (diamonds) in the UZC- τ -SALF and in the mock τ CDM-SALF redshift surveys.

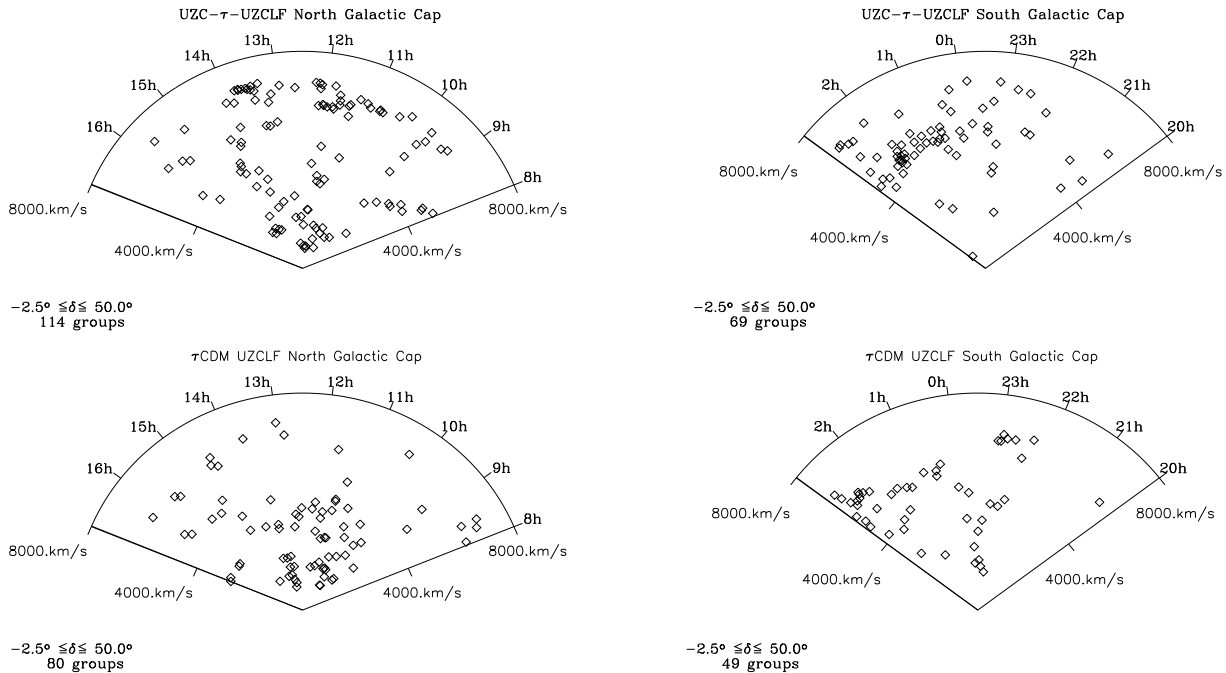


Figure 9. The distribution of groups (diamonds) in the UZC- τ -UZCLF and in the mock τ CDM-UZCLF redshift surveys.

is the main large-scale structure feature in the UZC. Unfortunately, the Great Wall, which is at $\sim 7000 \text{ km s}^{-1}$ from the Milky Way, is just on the border of our mock catalogues extracted from the constrained simulations. The mock catalogues do indeed show a concentration of galaxies at the location of the Great Wall, but this concentration appears substantially looser.

We compute below the two-point correlation functions of groups. However, this function is not exhaustive of the

large-scale structure description when the density field is not Gaussian, as in the case of the small UZC volume. Therefore, we provide here an alternative simple test of clustering.

Consider the space $\mathcal{S} = (\alpha, cz)$, the two-dimensional projection of the redshift space (α, δ, cz) . One can consider the galaxies as a random sample of an underlying density distribution N_{2D} in this space. If galaxy groups are fair tracers of the large-scale distribution of galaxies, we expect a positive Kolmogorov-Smirnov (KS) test between the distri-

Table 2. Total number of galaxies in the real and mock redshift surveys.

	SALF		UZCLF	
	UZC	Λ CDM	UZC	Λ CDM
NGC	5114	5037	5006	4979
SGC	2698	2667	2692	2566

	UZC	τ CDM	UZC	τ CDM
	NGC	4558	4621	5032
SGC	2623	2699	2693	2691

Table 3. Number of groups and fraction of galaxies in groups.

	SALF		UZCLF	
	UZC	Λ CDM	UZC	Λ CDM
NGC	114/0.27	118/0.35	114/0.26	85/0.24
SGC	69/0.28	63/0.34	69/0.28	51/0.18

	UZC	τ CDM	UZC	τ CDM
	NGC	101/0.23	70/0.16	114/0.27
SGC	68/0.28	34/0.11	69/0.28	49/0.15

butions of galaxies and groups in \mathcal{S} . Table 4 shows that this is indeed the case in the UZC, at a significance level larger than 17%. A large significance level is also provided by the Λ CDM model, whereas the τ CDM groups trace poorly the large-scale distribution of galaxies in most cases. For both models the situation moderately improves when the UZC luminosity function is used, except for the NGC of the Λ CDM model. This disagreement is not due to the difficulty of reproducing the Great Wall, because cutting the catalogues at 6000 km s^{-1} does not substantially improve the agreement.

Now, if N_{2D} in the models is comparable to N_{2D} in the UZC, we also expect a positive KS test between the models and the observations. The KS test applied to the galaxy N_{2D} fails because the initial conditions of the simulation are not set to reproduce the observed galaxy distribution on scales smaller than $5h^{-1}$ Mpc. However, groups trace the large scale distribution of galaxies fairly enough, and the comparison between the N_{2D} of the groups in the UZC and in the models is appropriate. Table 5 shows that the KS tests fail when we consider the entire survey region; however, the significance levels increase when we limit the region to 6000 km s^{-1} , therefore excluding the Great Wall.

Table 4. Groups of galaxies as tracers of the large-scale structure.

	SALF		UZCLF	
	UZC	Λ CDM	UZC	Λ CDM
NGC	0.17/0.65	0.11/0.07	0.25/0.54	0.03/0.08
SGC	0.22/0.18	0.32/0.13	0.23/0.19	0.37/0.20

	UZC	τ CDM	UZC	τ CDM
	NGC	0.19/0.45	0.002/0.01	0.23/0.56
SGC	0.29/0.23	0.02/0.03	0.23/0.18	0.21/0.24

Significance levels of the bidimensional KS test in the $\alpha - cz$ plane between the distributions of galaxies and groups in the range $cz \in [500, 7000] / [500, 6000] \text{ km s}^{-1}$.

Table 5. Comparison between the large scale distribution of the UZC and the simulated groups.

	SALF		UZCLF	
	Λ CDM	τ CDM	Λ CDM	τ CDM
NGC	3e-4/0.06	9e-8/0.03	2e-5/0.01	1e-4/0.01
SGC	2e-3/2e-3	3e-4/1e-3	4e-3/0.01	0.04/0.01

Bidimensional KS test in the $\alpha - cz$ plane between the distributions of groups in the UZC and the models in the range $cz \in [500, 7000] / [500, 6000] \text{ km s}^{-1}$.

Table 6. Number of galaxies brighter than $-19.02 + 5 \log h$ in the volume-limited catalogues.

	SALF		UZCLF	
	UZC	Λ CDM	UZC	Λ CDM
NGC	1788	1936	1788	1431
SGC	941	1011	941	479

	UZC	τ CDM	UZC	τ CDM
	NGC	1788	1823	1788
SGC	941	875	941	655

We finally consider groups in volume-limited catalogues (Table 6). The Λ CDM model agrees with the UZC better than the τ CDM model, which yields extremely low numbers of groups (Table 7).

All these results suggest that the structures in the Λ CDM model are better defined than those in the τ CDM model, although the agreement with the UZC is not yet satisfactory. The use of the UZC luminosity function alleviates some problems but it is clearly not the only relevant ingredient.

5.1 The correlation function of galaxies and groups

In the redshift space of the local Universe, the vector $\mathbf{s}_i = cz_i \mathbf{r}_i$ locates a galaxy with redshift $z_i \ll 1$ and celestial coordinates $\mathbf{r}_i = (\alpha_i, \delta_i)$. For small angular separations (smaller than 50° in our analysis), the components along the line of sight (π) and projected onto the sky (r_p) of the pairwise galaxy separation $\mathbf{s} = \mathbf{s}_i - \mathbf{s}_j$ are

$$\pi = \frac{\mathbf{s} \cdot \mathbf{l}}{|\mathbf{l}|}, \quad r_p^2 = s^2 - \pi^2, \quad (2)$$

Table 7. Number of groups and fraction of galaxies in groups for the volume-limited catalogues.

	SALF		UZCLF	
	UZC	Λ CDM	UZC	Λ CDM
NGC	18/0.08	15/0.09	18/0.08	7/0.06
SGC	17/0.15	15/0.13	17/0.15	1/0.01

	UZC	τ CDM	UZC	τ CDM
	NGC	18/0.08	3/0.01	18/0.08
SGC	17/0.15	0/0	17/0.15	1/0.01

where $\mathbf{l} = (\mathbf{s}_i + \mathbf{s}_j)/2$. The two-dimensional redshift space correlation function $\xi(r_p, \pi)$ measures the excess probability, compared to a Poisson distribution, that a galaxy pair has separation (r_p, π) . To measure $\xi(r_p, \pi)$, we compute the distribution of pair separations in the data and in a Poisson realization of the data with the same radial and angular selection criteria

$$\xi(r_p, \pi) = \frac{DD(r_p, \pi) n_R}{DR(r_p, \pi) n_D} - 1, \quad (3)$$

where DD and DR are the weighted sums (see below) of the data/data and data/random pairs with separation r_p and π , and n_D and n_R are the mean densities of the real and random samples, respectively.

The points in the random sample are radially distributed according to the selection function

$$\varphi(z) = \frac{\int_{-\infty}^{M(z)} \phi(M) dM}{\int_{-\infty}^{M(z_{\min})} \phi(M) dM}, \quad (4)$$

where the luminosity function $\phi(M)$ has the parameters, appropriate to the model considered, listed in Table 1. We consider only galaxies and groups in the range $cz = [500, 7000]$ km s⁻¹. $M(z_{\min})$ is the absolute magnitude corresponding to m_{lim} at the fiducial minimum redshift $cz_{\min} = 500$ km s⁻¹; $M(z)$ is the absolute magnitude corresponding to m_{lim} at any given redshift z . We constrain $M(z)$ to be brighter than the luminosity resolution of the corresponding catalogue. We adopt the usual assumption that the group and galaxy selection functions coincide (Ramella, Geller & Huchra 1990; Frederic 1995b; Trasarti-Battistoni et al. 1997; Girardi et al. 2000).

In magnitude-limited samples, the pair sums DD and DR are weighted to correct for the rapid decrease of the galaxy density with distance. In its simplest form, the weight is given by the inverse of the selection function $\varphi(z)$. A more appropriate approach, that we apply here, is the minimum-variance estimate (Davis & Huchra 1982). This approach requires the *a-priori* knowledge of the volume integral of the real-space correlation function $\xi(r)$. However, the weights are robust against different choices of $\xi(r)$; moreover, because this choice affects each catalogue in the same way, the conclusions of our comparison remain unchanged. We adopt a power-law correlation function $\xi(r) = (r/r_0)^{-\gamma}$, with $r_0 = 5.8h^{-1}$ Mpc and $\gamma = 1.8$ for both galaxies and groups.

Figure 10 shows the $\xi(r_p, \pi)$ maps of our SALF and UZCLF galaxy catalogues. These figures clearly show that the models have a substantially weaker clustering at large r_p and small π . This quantifies the lack of large and coherent structures. The Finger-of-Gods features (at large π and small r_p) are instead well reproduced, a result that indicates that the virial regions of clusters are correctly represented in the models.

We also compute the two-point redshift-space correlation function $\xi(s)$, where the separation s is

$$s = \frac{c}{H_0} \sqrt{z_i^2 + z_j^2 - 2z_i z_j \cos \theta_{ij}}, \quad (5)$$

and θ_{ij} is the angular separation of the two objects (galaxies or groups) with redshift z_i and z_j . $\xi(s)$ is more appropriate to quantify the clustering of groups, because the small number of objects makes $\xi(r_p, \pi)$ too noisy. To improve the

Table 8. Fit parameters of the redshift-space correlation function of galaxies.

	s_0 h^{-1} Mpc	γ
UZC- Λ -SALF	7.3 ± 0.3	1.18 ± 0.01
Λ CDM-SALF	5.5 ± 0.1	1.63 ± 0.01
UZC- Λ -UZCLF	7.3 ± 0.2	1.19 ± 0.01
Λ CDM-UZCLF	5.4 ± 0.1	1.67 ± 0.01
UZC- τ -SALF	7.1 ± 0.2	1.19 ± 0.01
τ CDM-SALF	5.1 ± 0.1	1.25 ± 0.01
UZC- τ -UZCLF	7.3 ± 0.3	1.18 ± 0.01
τ CDM-UZCLF	5.0 ± 0.2	1.25 ± 0.01

Table 9. Fit parameters of the redshift-space correlation function of groups with 3 or more members.

	s_0 h^{-1} Mpc	γ
UZC- Λ -SALF	6.9 ± 1.0	1.37 ± 0.03
Λ CDM-SALF	6.0 ± 1.0	1.39 ± 0.04
UZC- Λ -UZCLF	6.9 ± 1.0	1.38 ± 0.03
Λ CDM-UZCLF	7.5 ± 0.8	1.65 ± 0.03
UZC- τ -SALF	6.8 ± 1.0	1.40 ± 0.03
τ CDM-SALF	14.5 ± 2.0	1.15 ± 0.02
UZC- τ -UZCLF	6.9 ± 1.0	1.38 ± 0.03
τ CDM-UZCLF	7.4 ± 1.1	1.49 ± 0.04

statistics, we include systems with three or more members when computing the group $\xi(s)$.

To estimate the uncertainties we use a bootstrap procedure with 50 resampled samples in the case of galaxies and 400 in the case of groups.

Figures 11 and 12 show $\xi(s)$ for galaxies and groups. The fits $\xi(s) = (s/s_0)^{-\gamma}$ in the interval $2 - 10h^{-1}$ Mpc for each model are summarized in Tables 8 and 9.

Our results confirm the measure of $\xi(s)$ by Mathis et al. (2002) (our Figure 11 is equivalent to their Figure 16): the τ CDM model provides a galaxy $\xi(s)$ which is systematically lower than the UZC $\xi(s)$ by a factor 0.6 to 3. The Λ CDM model provides a much better match on scales smaller than $5h^{-1}$ Mpc, whereas its $\xi(s)$ is up to a factor 2 smaller at larger scales. We remind that the initial conditions are drawn from the IRAS 1.2 Jy survey rather than from the UZC optically-selected galaxies, and indeed Mathis et al. (2002) show that the $\xi(s)$'s of the model and of the PSCz survey do agree on all scales in the Λ CDM model and on scales larger than $5h^{-1}$ Mpc in the τ CDM model. To compare the models with the PSCz correlation function, however, Mathis et al. (2002) assign a far-infrared luminosity to each galaxy by matching the simulated infrared luminosity function to the observed IRAS luminosity function, a procedure similar to the reassignment of the optical luminosities we apply to compile the UZCLF catalogues. Therefore, the fact that this by-hand luminosity assignments can yield satisfactory results in some bands but not in others suggests

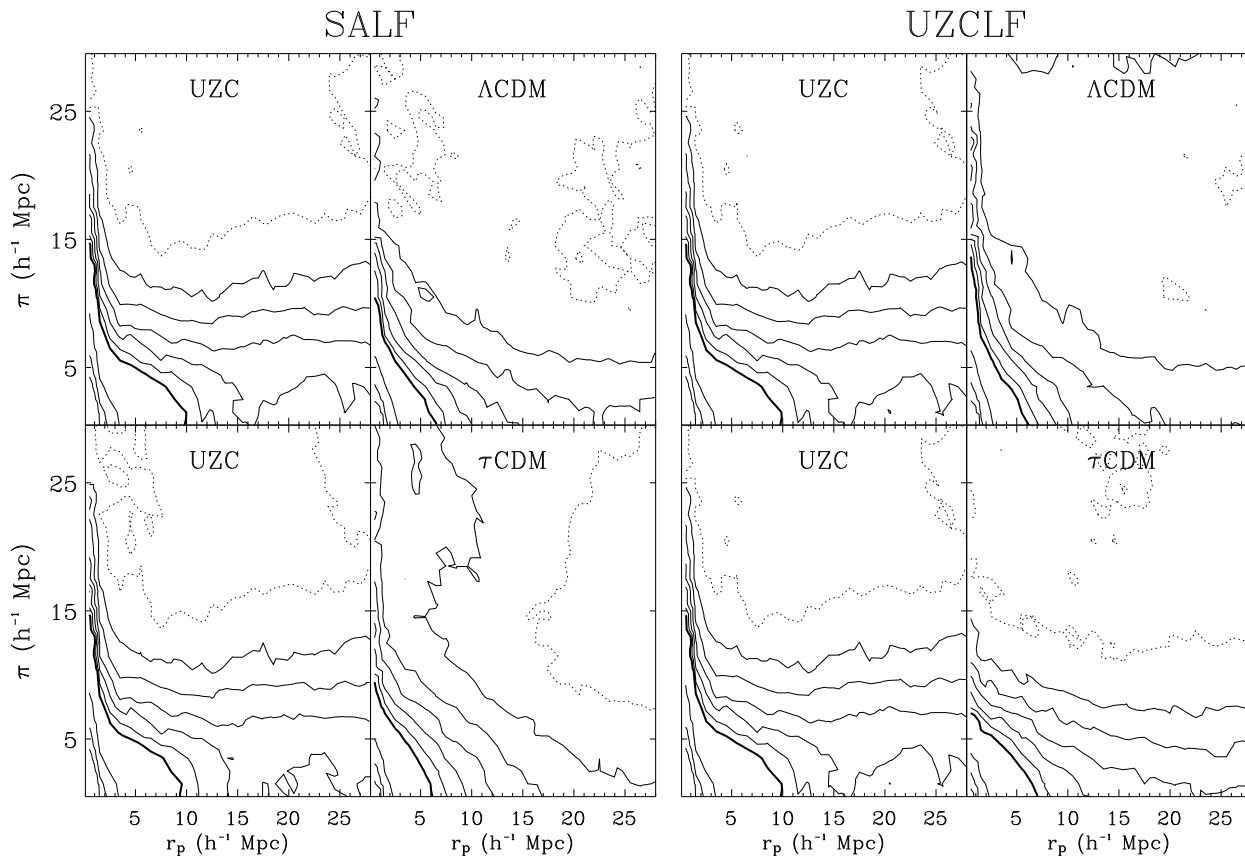


Figure 10. The galaxy two-dimensional redshift-space correlation function $\xi(r_p, \pi)$. The bold contour indicates $\xi(r_p, \pi) = 1$. The contour levels are separated by logarithmic intervals of 0.2 for $\xi(r_p, \pi) > 1$ and by linear intervals of 0.2 for $\xi(r_p, \pi) < 1$. The dotted contours show $\xi(r_p, \pi) < 0$.

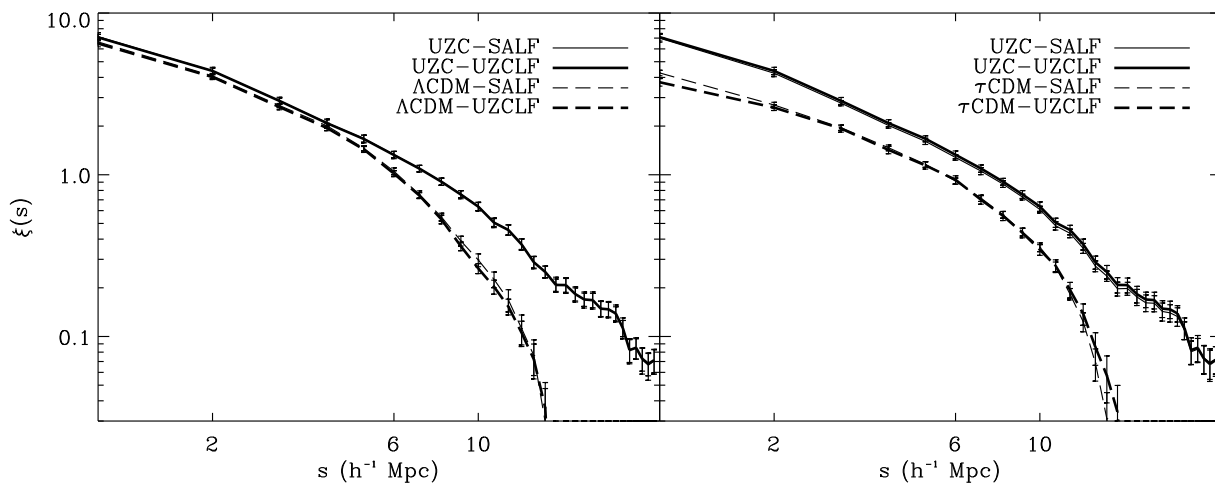


Figure 11. The galaxy redshift-space correlation function. The error bars are $1\text{-}\sigma$ bootstrap errors.

that the clustering power of the underlying dark matter distribution is probably correct, whereas the model describing how galaxies acquire their luminosity in the various bands has to be improved.

Unlike the galaxy $\xi(s)$, the group $\xi(s)$ depends on the adopted optical luminosity function. $\Lambda\text{CDM-SALF}$ model

is in better agreement with observations than the $\Lambda\text{CDM-UZCLF}$, which tends to give a higher degree of clustering on smaller scales; in any case both models agree with the UZC $\xi(s)$ within the errors. The $\tau\text{CDM-UZCLF}$ model also agrees with observations, whereas the $\tau\text{CDM-SALF}$ is at least $2\text{-}\sigma$ above the UZC. The higher degree of clustering of

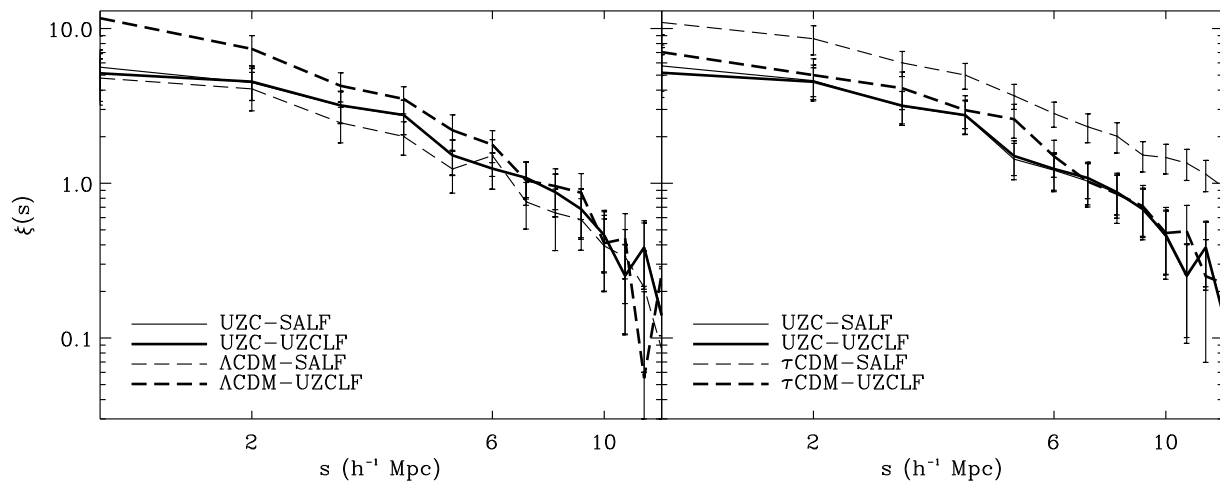


Figure 12. The group redshift-space correlation function. The error bars are $1\text{-}\sigma$ bootstrap errors.

the τ CDM-SALF model is a consequence of the fact that most groups reside in the nearby region around Virgo (see Figure 8).

Our results show that the amplitude of the UZC group correlation function is smaller than or equal to the amplitude of the galaxy correlation function (Jing & Zhang 1988; Ramella et al. 1990). This lower amplitude is confirmed in the much larger group sample extracted from the 2dF survey (Padilla et al. 2004). Other work suggests instead that groups in small (Girardi et al. 2000; Giuricin et al. 2001; Padilla et al. 2001) and large samples (Zandivarez, Merchán & Padilla 2003) are more clustered than galaxies. Most of this disagreement however is likely to be due to the fact that many poor groups are spurious and decrease the amplitude of $\xi(s)$ toward the $\xi(s)$ of field galaxies. Indeed the normalization s_0 systematically increases with the exclusion of groups with fewer and fewer members (Padilla et al. 2004). In fact, we also find that, in the UZC, the $\xi(s)$ of groups with at least five members has $s_0 = 8.8 \pm 2.1 h^{-1} \text{Mpc}$ and $\gamma = 1.30 \pm 0.05$, and is larger than that of galaxies.

6 THE LIGHT DISTRIBUTION IN THE NEARBY UNIVERSE

In this section we investigate the luminosity content of individual groups. We study the group luminosity function, the mass-to-light ratio, the halo occupation number and the light distribution among galaxy members.

6.1 The luminosity function and abundances of groups

To estimate the space density of redshift-space groups we weight each group by $1/\Gamma_{\text{max}}$, where

$$\Gamma_{\text{max}} = \frac{\omega}{3} \left(\frac{cz_5}{H_0} \right)^3 \left[1 - \frac{3cz_5}{2}(1+q_0) \right] \quad (6)$$

is the volume sampled by the group. In fact, cz_5/H_0 is the smallest distance between our group distance cut off

7000 km s^{-1} and the maximum distance beyond which the fifth brightest galaxy member would be fainter than the apparent magnitude limit m_{lim} ; moreover, ω is the solid angle of the catalogue, c the light speed, and q_0 the deceleration parameter which we suppose to be unknown and set equal to 0.5. This choice is irrelevant, because, for the small distances considered here, the correct value $q_0 = -0.55$ for the Λ CDM model yields a Γ_{max} which differs by less than 3 per cent from the Γ_{max} estimated with $q_0 = 0.5$.

In real space, we consider a group each dark matter halo containing $N \geq 5$ members brighter than the appropriate luminosity resolution. We compute the total luminosity L_{tot} of a real-space group as the sum of the luminosities of the N resolved galaxies within the halo, $L_{\text{gal}} = \sum_i L_i$, and the luminosity of the galaxies fainter than the luminosity resolution limit L_{lim}

$$L_{\text{faint}} = \frac{N}{\int_{L_{\text{lim}}}^{\infty} \phi(L) dL} \times \int_0^{L_{\text{lim}}} \phi(L) L dL, \quad (7)$$

where $\phi(L)$ is the adopted galaxy luminosity function.

In redshift space, we use the same equations with the only difference that the luminosity resolution limit L_{lim} is replaced by the brightest luminosity between the luminosity resolution and the absolute magnitude $M_{\text{lim}} = m_{\text{lim}} - 25 - 5 \log(\langle cz \rangle / H_0)$, where $\langle cz \rangle / H_0$ is the group distance.

Not surprisingly, Figure 13 shows that neither the Λ CDM- nor the τ CDM-SALF mock catalogues reproduce the UZC group luminosity function. With the UZCLF catalogues the situation improves, but it is still unsatisfactory, because the KS and Wilcoxon-Rank-Sum (WRS) tests indicate that the mock distributions are not drawn from the same population of the UZC at very high significance levels (Tables 11 and 12).

Nevertheless the Λ CDM-UZCLF appears to yield a luminosity function closer to the UZC than the τ CDM-UZCLF. In fact, the τ CDM model fails at providing numerous enough luminous groups, despite the fact that the τ CDM model produces a number of bright galaxies larger than both the Λ CDM model and the UZC (Figure 1). However, the small amplitude of the galaxy two-point correlation function (Figure 11) shows that the galaxies are not

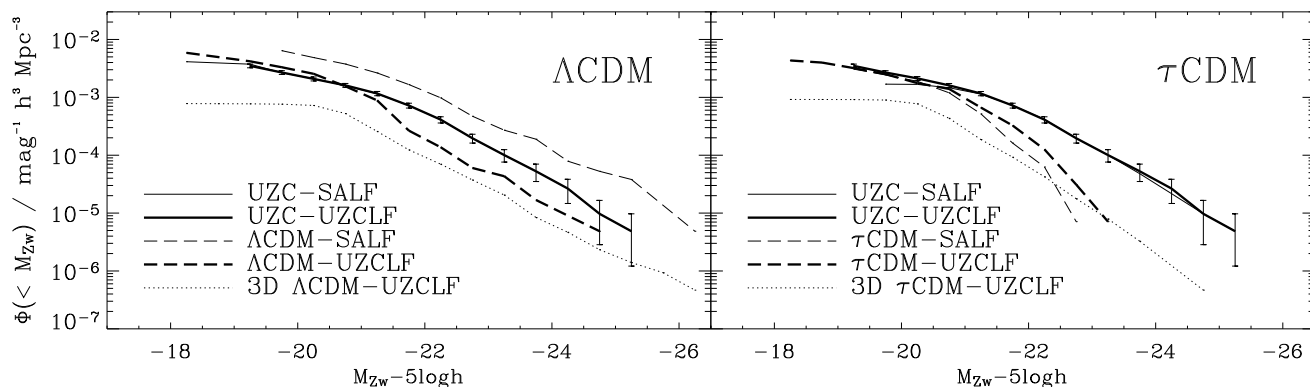


Figure 13. Cumulative luminosity function. The error bars are $1\text{-}\sigma$ Poisson errors and are only shown for the UZC for clarity. The error bars for the models have similar size.

enough clustered to yield either a sufficiently large fraction of galaxies in groups or a sufficiently large number of groups. Consequently, the median luminosities of the τ CDM groups are lower than in the UZC (Table 10).

Figure 14 shows the abundances of groups by harmonic radius

$$R_h = \frac{\pi \langle cz \rangle}{2 H_0} N(N-1) \left[\sum_{i=1}^{N-1} \sum_{j=i+1}^N \frac{1}{\tan(\theta_{ij}/2)} \right]^{-1}, \quad (8)$$

where N is the number of members and θ_{ij} are the pairwise angular separations, velocity dispersion

$$\sigma = \left[\frac{1}{N-1} \sum_{i=1}^N (cz_i - \langle cz \rangle)^2 \right]^{1/2} \quad (9)$$

and virial mass

$$M_{\text{vir}} = \frac{6\sigma^2 R_h}{G}. \quad (10)$$

To avoid divergences, we set, according to Ramella (private communication), $\tan(\theta_{ij}/2)\langle cz \rangle/H_0 = r_{ij} = 0.03h^{-1}$ Mpc when $r_{ij} < 0.03h^{-1}$ Mpc. The SALF catalogues perform very poorly: the medians of these quantities are sensibly different from the UZC medians (Table 10) and the KS and WRS tests indicate that the mock groups and the UZC groups are certainly drawn from different parent populations (Tables 11 and 12). The only exceptions are the σ and M_{vir} distributions of the τ CDM models and the $M_{\text{vir}}/L_{\text{tot}}$ distribution of the Λ CDM model.

The UZCLF catalogues perform substantially better: with the exception of the L_{tot} and $M_{\text{vir}}/L_{\text{tot}}$ distributions, both the Λ CDM and the τ CDM models provide a rather good match to the UZC group abundances, with the Λ CDM model yielding the largest significance levels.

Figure 14 also shows the number density of the groups in real space (dotted lines). For these groups

$$R_h = \frac{N(N-1)}{2} \left[\sum_{i=1}^{N-1} \sum_{j=i+1}^N \frac{1}{|\mathbf{r}_{ij}|} \right]^{-1}, \quad (11)$$

where \mathbf{r}_{ij} are the pairwise separations,

$$\sigma = \left[\frac{1}{3(N-1)} \sum_{i=1}^N (\mathbf{v}_i - \langle \mathbf{v} \rangle)^2 \right]^{1/2} \quad (12)$$

and $M_{\text{vir}} = 6\sigma^2 R_h/G$.

In the Λ CDM model, the number densities of groups estimated in redshift space are larger than the real-space number densities, whereas in the τ CDM model the largest discrepancy appears in the number density by harmonic radius. This result agrees with the fact that R_h can be overestimated by a factor as large as two because of the presence of interlopers (Diaferio et al. 1999). In the virial mass estimation, however, this bias is less relevant than the bias on σ , because of the different powers that R_h and σ have in the virial mass relation: on the scale of clusters, where σ is almost unbiased, the recovered mass function is in reasonable agreement with the real-space mass function.

N -body simulations, where galaxies were identified as density peaks (Nolthenius & White 1987; Moore, Frenk & White 1993; Frederic 1995a,b) or formed and evolved with semi-analytic prescriptions (Diaferio et al. 1999), show that the FOF algorithm generally returns groups with statistical properties comparable to those of the real-space groups; however, interlopers and spurious groups can severely affect the estimates of the intrinsic properties of individual groups and this bias is more dramatic for groups with fewer members (Diaferio et al. 1999; Eke et al. 2004b; Berlind et al. 2006). Figure 14 shows that the discrepancy between the average properties of real- and redshift-space groups might be larger than usually assumed.

Recently, group-finder algorithms alternative to the FOF have been proposed and might identify real-space groups more accurately than the FOF algorithm (Eke et al. 2004a; Yang et al. 2005b). However, the FOF algorithm has been traditionally applied to the UZC and we use it here to make our results easily comparable to previous work. Moreover, we are interested in the comparison between models and observations when they are both analyzed with the same technique, rather than in the determination of the most reliable group finder. It is indeed a relevant result that the UZCLF catalogues agree with the UZC remarkably well, despite the fact that the recover of the average properties of

Table 10. Median values of the group properties.

	SALF		UZCLF	
	UZC/ Λ CDM/3D	UZC/ τ CDM/3D	UZC/ Λ CDM/3D	UZC/ τ CDM/3D
R_h	0.42 / 0.64 / 0.29	0.42 / 0.51 / 0.28	0.42 / 0.44 / 0.29	0.42 / 0.47 / 0.28
σ	219 / 284 / 230	222 / 217 / 320	219 / 217 / 230	217 / 250 / 320
$\log M_{\text{vir}}$	13.45 / 13.81 / 13.29	13.48 / 13.54 / 13.57	13.45 / 13.44 / 13.29	13.45 / 13.59 / 13.57
$\log L_{\text{tot}}$	10.88 / 11.07 / 10.58	10.92 / 10.56 / 10.65	10.88 / 10.64 / 10.49	10.88 / 10.64 / 10.38
$\log(M_{\text{vir}}/L_{\text{tot}})$	2.59 / 2.70 / 2.70	2.58 / 2.94 / 2.93	2.60 / 2.85 / 2.79	2.60 / 2.96 / 3.20
Ω_0	0.27 / 0.27 / -	0.27 / 0.82 / -	0.28 / 0.50 / -	0.28 / 0.64 / -

Median properties of the galaxy groups with more than five members. R_h , σ , M_{vir} , L_{tot} and $M_{\text{vir}}/L_{\text{tot}}$ are in units of h^{-1} Mpc, km s^{-1} , $h^{-1}M_{\odot}$, $h^{-2}L_{\odot}$ and hM_{\odot}/L_{\odot} , respectively.

Table 11. Comparison of the UZC and the mock group abundances: KS test.

	SALF		UZCLF	
	Λ CDM	τ CDM	Λ CDM	τ CDM
R_h	10^{-9}	10^{-3}	0.15	0.14
σ	10^{-3}	0.10	0.27	0.08
$\log M_{\text{vir}}$	10^{-5}	0.11	0.34	0.02
$\log L_{\text{tot}}$	10^{-5}	10^{-11}	10^{-7}	10^{-5}
$\log(M_{\text{vir}}/L_{\text{tot}})$	0.15	10^{-11}	10^{-4}	10^{-9}

Significance levels of the KS test for the null hypothesis that the UZC and the mock groups are drawn from the same parent population.

Table 12. Comparison of the UZC and the mock group abundances: WRS test.

	SALF		UZCLF	
	Λ CDM	τ CDM	Λ CDM	τ CDM
R_h	0	10^{-3}	0.16	0.04
σ	10^{-3}	0.39	0.41	0.03
$\log M_{\text{vir}}$	10^{-6}	0.25	0.29	0.01
$\log L_{\text{tot}}$	10^{-5}	0	10^{-7}	10^{-6}
$\log(M_{\text{vir}}/L_{\text{tot}})$	0.01	0	10^{-6}	0

Significance levels of the Wilcoxon Rank-Sum (WRS) test for the null hypothesis that the UZC and the mock groups are drawn from the same parent population.

the real-space groups with the FOF algorithm is only partially correct.

6.2 Mass-to-light ratio vs. mass

Figure 15 shows that the mass-to-light ratio $M_{\text{vir}}/L_{\text{tot}}$ of the UZC groups increases with mass, as other samples of groups have already demonstrated (Marinoni & Hudson 2002; Lanzoni et al. 2004; Eke et al. 2004b, 2006). Semi-analytic models of galaxy formation show that the dependence of $M_{\text{vir}}/L_{\text{tot}}$ on mass naturally arises in hierarchical models (Kauffmann et al. 1999; Benson et al. 2000), and extensions of the halo model use this relation as a sensitive probe to constrain the efficiency of galaxy formation and the normalization of the power spectrum of the primordial density fluctuations σ_8 (van den Bosch et al. 2003b; Tinker et al. 2005).

The universal value of the mass-to-light ratio is $\langle M/L \rangle = \rho_{\text{crit}}\Omega_0/j$, where ρ_{crit} is the critical density of the Universe and $j = \phi^*L^*\Gamma(\alpha + 2)$ is the luminosity density derived from the galaxy luminosity function. In our models, the real-space relations approaches a universal value at sufficiently large masses; this value does not correspond to the correct Ω_0 , however, because the virial mass M_{vir} estimated in real space is still $\sim 30 - 40\%$ larger than the actual mass of the dark matter halo (Diaferio et al. 1999). In redshift space the $M/L - M$ relations do not clearly show this flattening, but their rather large percentile ranges include the real-space relations. The Λ CDM model matches the UZC results rather well, whereas the τ CDM model provides too large mass-to-light ratios both because it does not provides luminous groups and because the real Universe seems to have a low value of Ω_0 and, consequently, a low value of $\langle M/L \rangle$.

6.3 Halo occupation number

The halo occupation number (HON) is the mean number of galaxies brighter than a luminosity threshold in dark matter halos of a given mass; it quantifies how efficient galaxy formation is in halos of different masses (Kauffmann et al. 1997; Benson et al. 2000; Scoccimarro et al. 2001; van den Bosch et al. 2003a; Berlind et al. 2003; Kravtsov et al. 2004; Zheng et al. 2005). With appropriate extensions, one can use the HON to model the dependence of galaxy properties on environment (Yang et al. 2005a; Sheth 2005; Skibba et al. 2006; Sheth et al. 2006).

Estimating the HON of real systems requires accurate photometry and accurate determination of the total mass and galaxy membership. To avoid these difficulties, a common approach is to assume an analytic form for the HON and adjust its parameters to match the observed galaxy two-point correlation function (Jing et al. 1998; Magliocchetti & Porciani 2003; Abazajian et al. 2004; Zehavi et al. 2005). Alternatively, one can directly use the galaxy luminosity function to estimate the expected number of galaxies in the cluster volume (Marinoni & Hudson 2002; Lin et al. 2004).

These approaches have provided an indirect comparison of the observed HON with N -body or semi-analytic simulations. A direct comparison requires galaxy counts for a sample of galaxy systems (Kochanek et al. 2003, Lin et al. 2004, Popesso et al. 2006). One of these direct counts was

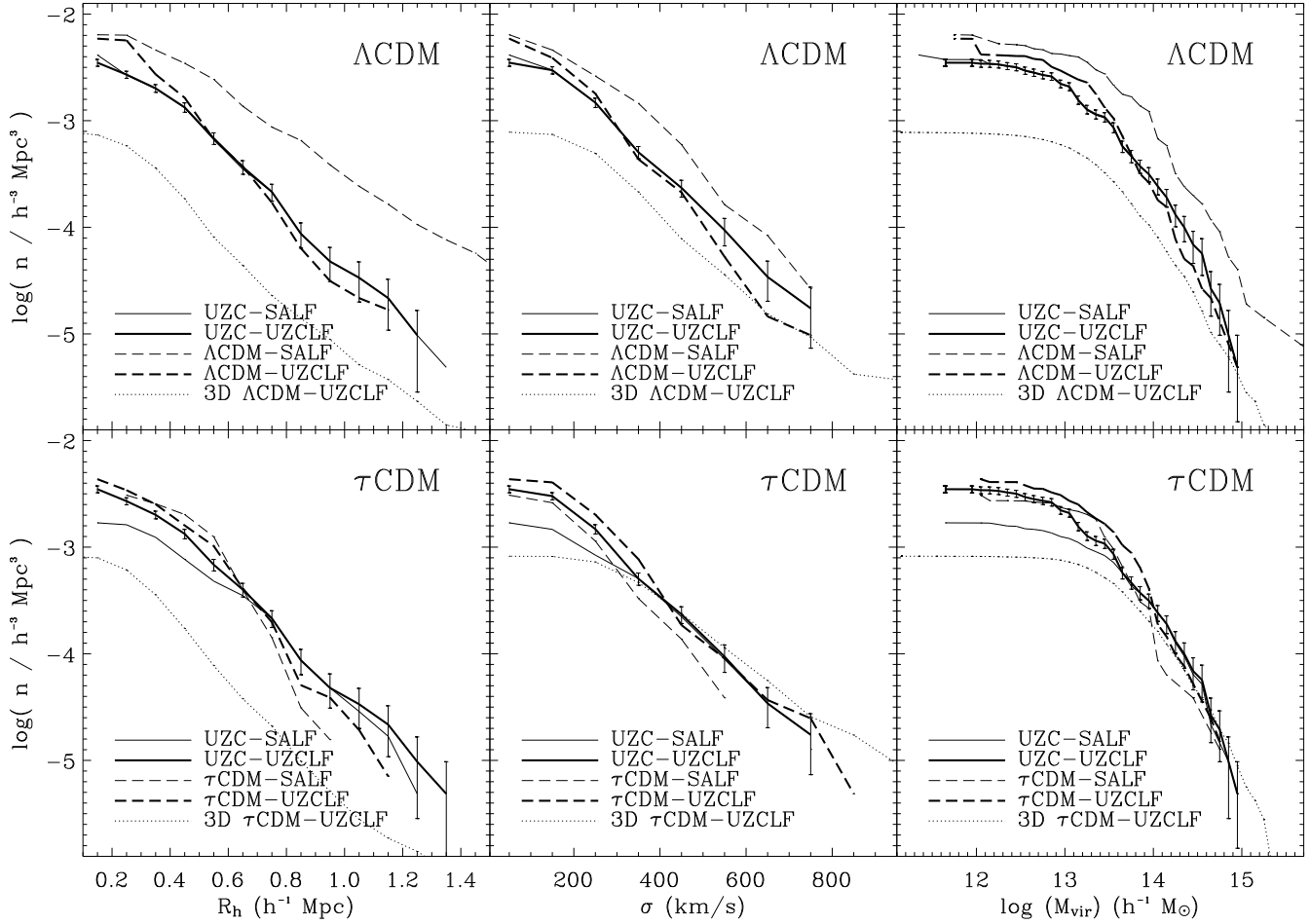


Figure 14. Cumulative number density of groups by harmonic radius R_h , velocity dispersion σ , and virial mass M_{vir} . The error bars are $1\text{-}\sigma$ Poisson errors and are only shown for the UZC for clarity. The error bars for the models have similar size.

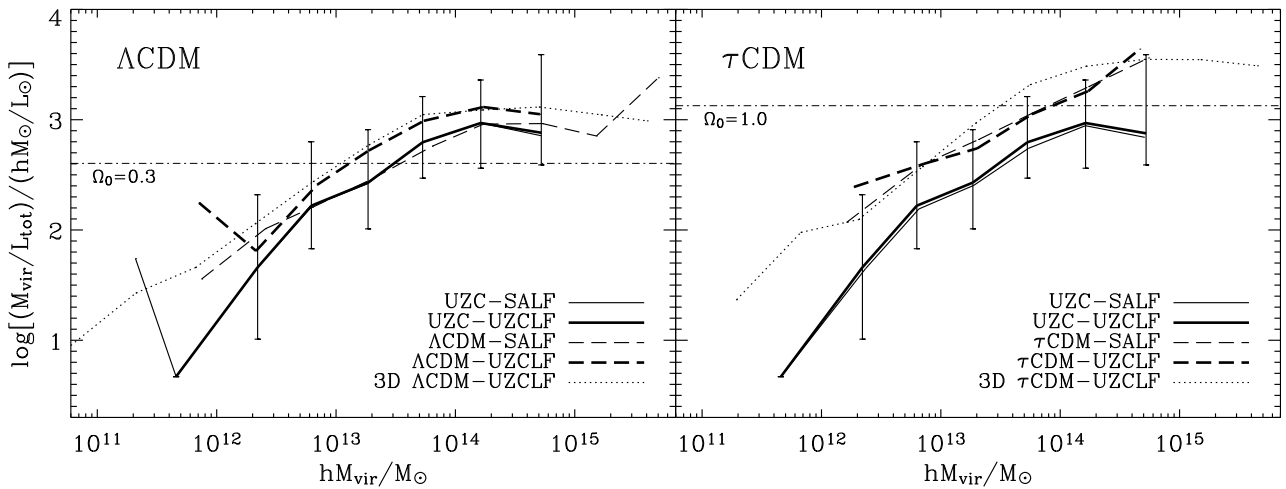


Figure 15. Group mass-to-light ratio vs. virial mass. The lines connect the medians of each bin and the error bars, only shown for the UZC for clarity, indicate the 0.1 and 0.9 percentiles. The error bars for the models have similar size. The dot-dashed line shows the universal mass-to-light ratio in the model.

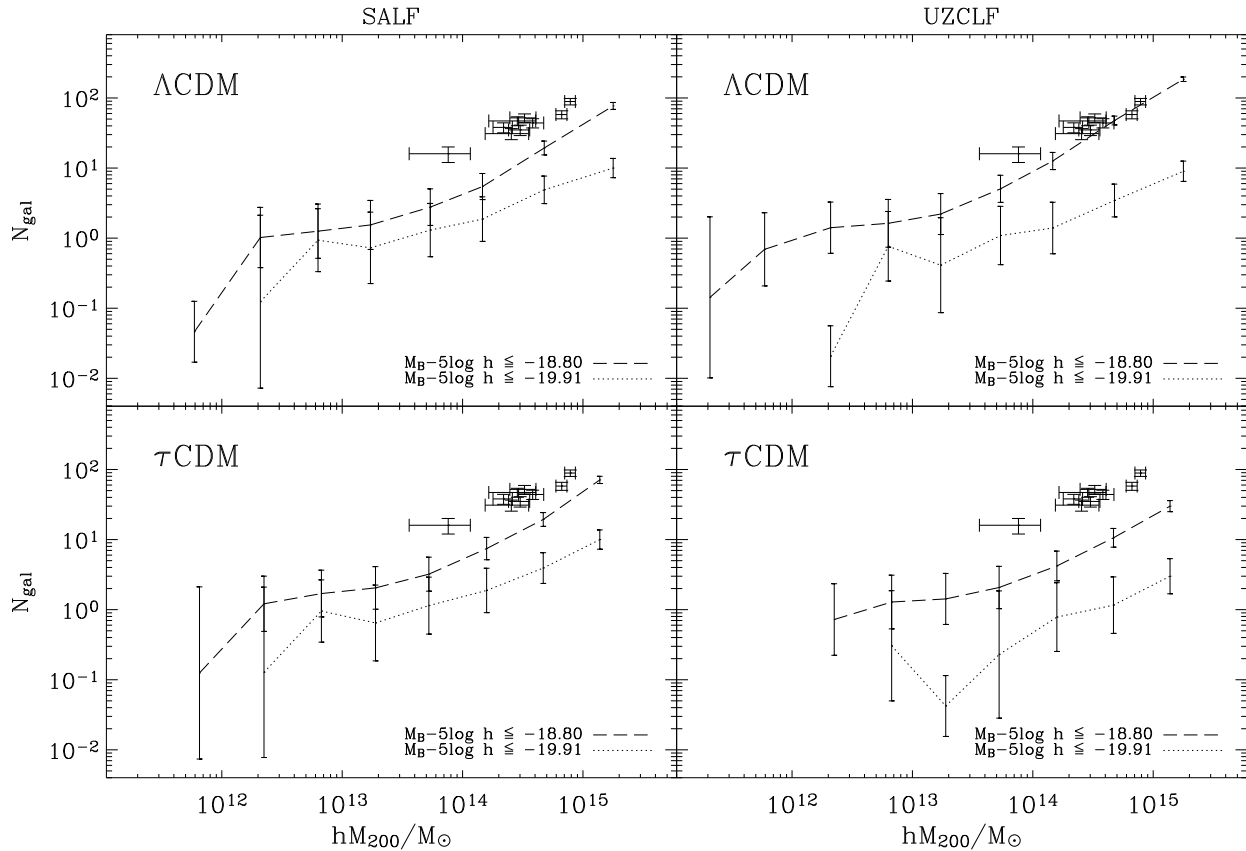


Figure 16. The halo occupation number (HON) in real space. The top (bottom) panels show the Λ CDM (τ CDM) model. In each panel lines are for galaxies brighter than $M_B - 5 \log h = -18.80$, and -19.91 (top to bottom) in the Λ CDM model, and -18.80 , and -19.91 (top to bottom) in the τ CDM model. The HON values smaller than one are due to haloes containing no galaxies brighter than the threshold. The error bars are $1\text{-}\sigma$ Poisson errors. The points with error bars on both axes show the nine CAIRNS clusters (Rines et al. 2004).

performed by Rines et al. (2004) for the nine CAIRNS clusters, thanks to their accurate 2MASS infrared photometry and spectroscopic uniform sky coverage. Figure 16 shows the CAIRNS cluster results.

Before comparing the HON of the UZC groups with the model groups, we check what model, if any, can reproduce the HON of these real clusters. This comparison is more robust than the comparison with groups, because the galaxy membership in groups is substantially more uncertain than in clusters, and the comparison between models and observations will be obscured by the large error bars (see Figure 17 below).

To compare the CAIRNS HON with the HON in the simulations we need to convert the 2MASS K_s -band to the B -band. According to Jarrett (2000), $B - K_s$ varies between 2.86 and 3.97, depending on the galaxy morphology; these colours have rms uncertainties in the range 0.30-0.80. Therefore, the luminosity limit imposed by Rines et al. (2004) lies in the B -band range $[-18.80, -19.91]$. Figure 16 shows the HON of the simulations in real space for both luminosity limits. Because early-type galaxies tend to reside in clusters and have redder colours, the fainter limit (dashed line) is probably the most appropriate for the comparison.

The SALF catalogues provide a factor of ~ 3 fewer

galaxies, whereas only the Λ CDM-UZCLF model provides a good match to the CAIRNS clusters. The slight underestimate still present in this case might originate from the fact that, because of the difficulties at identifying galaxy members, Rines et al. (2004) include all the galaxies projected onto the cluster.

When extending the comparison to the scales of groups, uncertainties on galaxy memberships and mass estimates become larger. Therefore, because the luminosity L_{tot} appears to be a more robust quantity than the virial mass M_{vir} (Eke et al. 2004b), we measure the HON as a function of both L_{tot} and M_{vir} (Figure 17). In general the models underestimate the UZC $N_{\text{gal}} - M_{\text{vir}}$ relation, regardless of the luminosity function adopted. On the contrary, the simulated $N_{\text{gal}} - L_{\text{tot}}$ relations agree well with the UZC, particularly the Λ CDM-UZCLF model. The τ CDM models reproduce the observed slope and normalization, but their relations vanish at large L_{tot} , because their mock surveys do not contain enough luminous groups.

6.4 The light distribution within groups

In the semi-analytic models analyzed here mergings between galaxies are allowed only when one of the two galaxies is

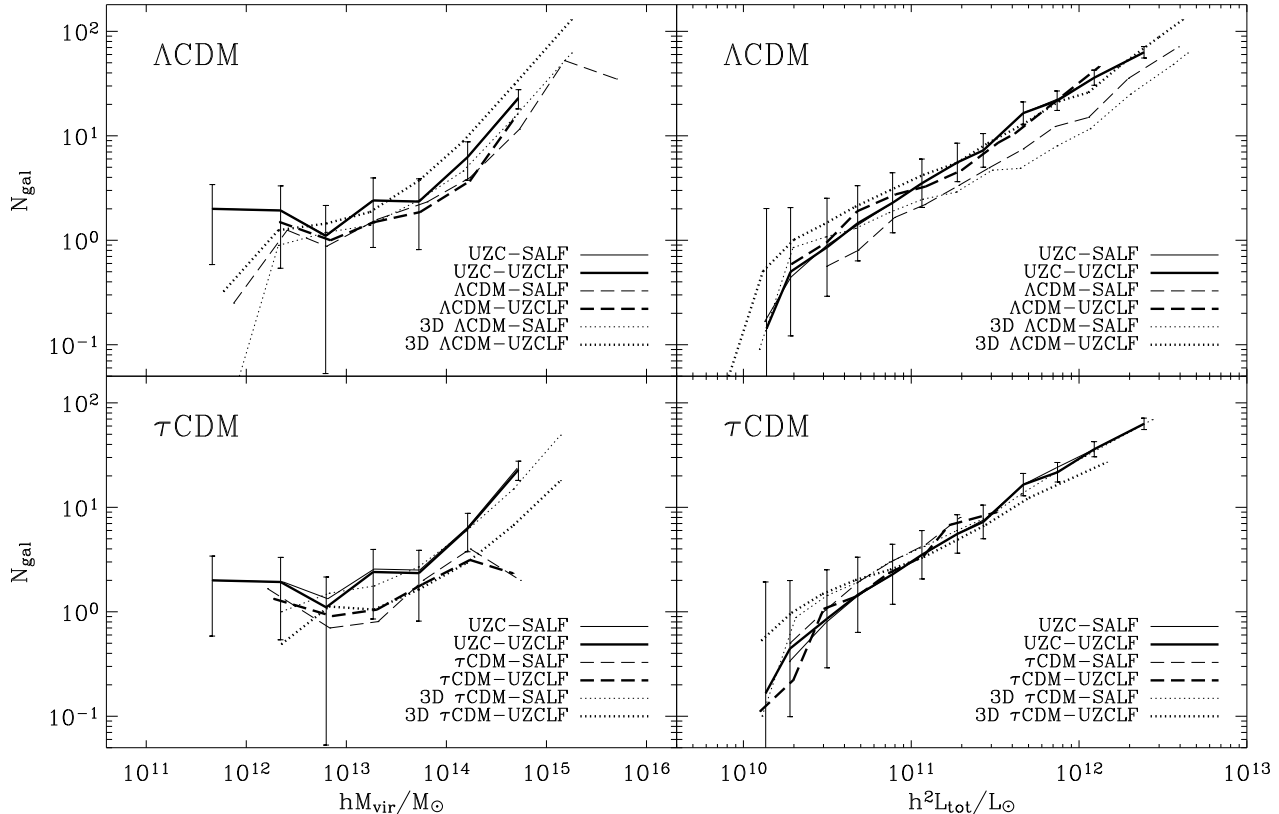


Figure 17. The halo occupation number (HON) in redshift space for groups with 5 or more members. The top (bottom) panels show the Λ CDM (τ CDM) model. The lines are for galaxies brighter than $M_B = -19.02 + 5 \log h$, the luminosity of a galaxy with apparent magnitude $m_{\text{lim}} = 15.5$ at the cut off distance 8000 km s^{-1} . The dotted lines are the real space HON at the same $M_B = -19.02 + 5 \log h$. The HON is shown as a function of group mass M_{vir} (left panels) and group total luminosity L_{tot} (right panels). The HON values smaller than one are due to haloes containing no galaxies brighter than the chosen threshold. The error bars are $1\text{-}\sigma$ Poisson uncertainties and are only shown for the UZC for clarity. The error bars for the models have similar size.

the central galaxy of the dark matter halo: satellite-satellite merging is not implemented. Moreover gas cooling is allowed only onto the central galaxy and satellite galaxies stop forming stars when their internal reservoir of cold gas is exhausted. These two processes yield a luminosity difference ΔL_{12} between the first and the second brightest galaxies in a group that can be substantially larger than observed.

In Figure 18 we plot ΔL_{12} as a function of the group total luminosity. The median ΔL_{12} is $3.3 \times 10^9 h^{-2} L_{\odot}$ for the UZC and $9.3 \times 10^9 h^{-2} L_{\odot}$ for the Λ CDM-SALF model. The ΔL_{12} density distribution of the τ CDM-SALF model is similar to the UZC (its median is $\Delta L_{12} = 3.7 \times 10^9 h^{-2} L_{\odot}$), but the tail of the high-luminosity groups is missing. To quantify the $L_{\text{tot}} - \Delta L_{12}$ relation, Table 13 lists the Spearman rank-order correlation coefficients r and their probability P : smaller P 's indicate stronger correlations. In the Λ CDM-SALF model, the correlation is orders of magnitude stronger than in the UZC. By reassigning the galaxy luminosity according to the UZC luminosity function the correlation weakens to the observed level.

The semi-analytic recipes produce many more bright galaxies than observed in the UZC (Figure 1). This fact can boost, in some cases, the luminosity difference ΔL_{12} , as one can see by comparing the two Λ CDM panels in Figure 18.

Table 13. Correlation between ΔL_{12} and the group total luminosity.

	SALF		UZCLF	
	UZC	Λ CDM	UZC	Λ CDM
r	0.30	0.63	0.29	0.33
P	10^{-4}	10^{-19}	10^{-4}	10^{-4}

	UZC	τ CDM	UZC	τ CDM
	r	0.31	0.35	0.29
P	10^{-4}	10^{-4}	10^{-4}	10^{-4}

Spearman rank correlation coefficient (r) and the significance of its deviation from zero (P). A smaller value of P indicates a stronger correlation.

We therefore also consider the ratio L_2/L_1 of the luminosities of the two brightest galaxies. The medians are 0.69 for the UZC and 0.52 and 0.63 for the Λ CDM-SALF and the τ CDM-SALF models, respectively, and confirm that the second brightest galaxy is on average fainter in the models than in the UZC.

A more quantitative comparison is obtained by considering the density distributions of the luminosity ratios. Table

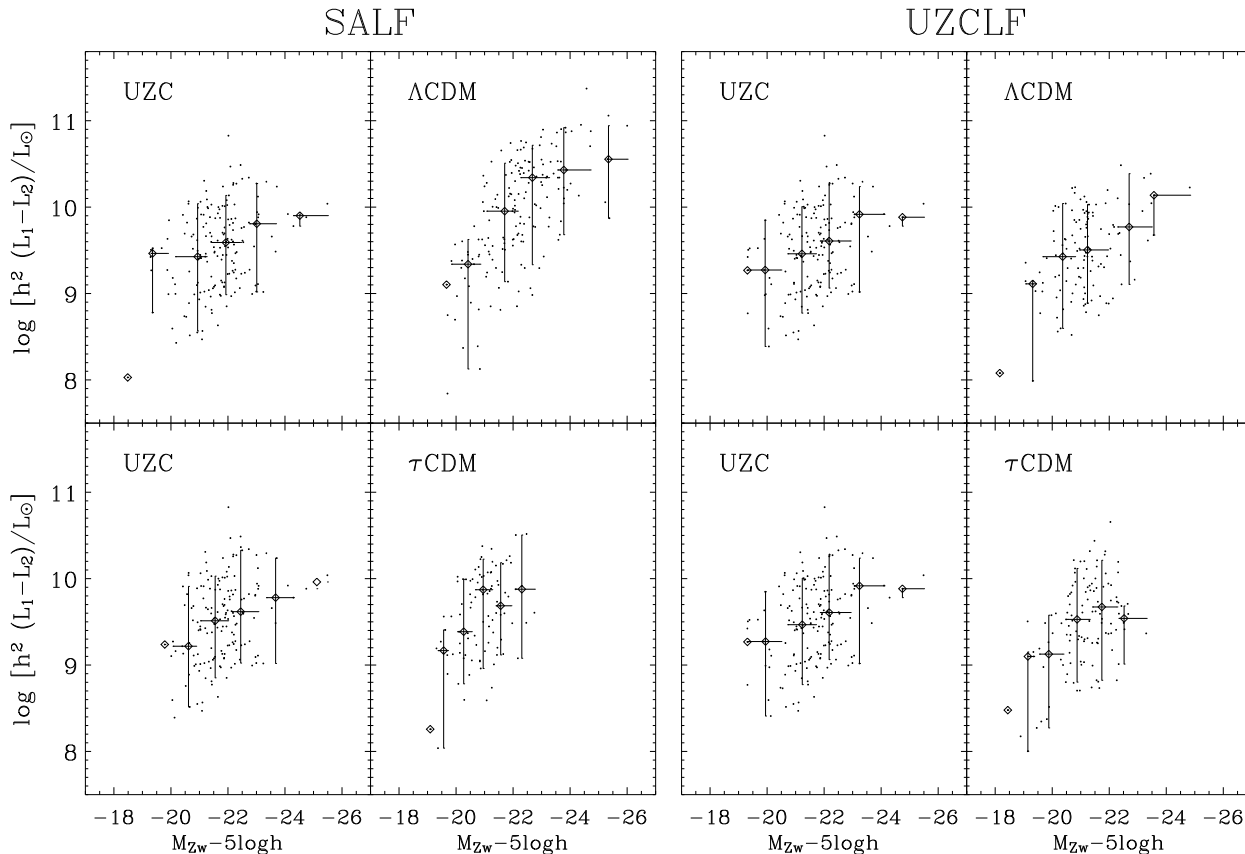


Figure 18. Luminosity difference between the first and the second rank galaxies in a group as a function of the group total luminosity.

Table 14. UZO-model comparison of the luminosity ratio between the two brightest galaxies in a group.

	SALF		UZCLF	
	Λ CDM	τ CDM	Λ CDM	τ CDM
KS	10^{-5}	0.01	0.78	0.67
WRS	10^{-7}	10^{-3}	0.41	0.38

Significance levels of the KS and WRS tests for the null hypothesis that the luminosity ratio L_2/L_1 between the second and first brightest galaxies in the UZO and in the simulated groups are drawn from the same parent population.

Table 14 lists the significance levels of the KS and WRS tests for the null hypothesis that the UZO and the model L_2/L_1 's are drawn from the same parent population. Clearly, the Λ CDM-SALF and the UZO groups have different parent populations, whereas the 1% significance level of the τ CDM-SALF is a consequence of the failure of this model to yield groups brighter than $M_B - 5 \log h \sim -22$, as we have clarified above (Figure 18). The comparison is instead satisfactory when the galaxy luminosities are reassigned according to the UZO luminosity function (UZCLF catalogues): both models now agree with the UZO to a significance level greater than 38%.

7 CONCLUSIONS

We have compared the properties of groups and clusters of galaxies extracted from the UZO (Falco et al. 1999) with those of systems extracted from mock redshift surveys. We have compiled these mock surveys from N -body simulations constrained to reproduce the large-scale distribution of galaxies in the nearby Universe (Mathis et al. 2002). In the simulations, galaxies are formed and evolved according to a semi-analytic procedure and we are thus able to constrain both the group clustering and the group luminosity content.

By using simulations with constrained initial conditions, we minimize the possible role played by cosmic variance, and differences between real and mock catalogues should mostly originate from the galaxy formation recipes. Our approach thus differs from previous attempts of comparing simulations with real group catalogues, where either cosmic variance was an issue (Diaferio et al. 1999) or the real catalog was large enough that cosmic variance was naturally suppressed (Eke et al. 2004a; Berlind et al. 2006).

The gross large-scale distribution of galaxies, including the location of the major nearby clusters, is very similar in the mock and real surveys, as mostly imposed by the initial conditions. However, the simulated large-scale structures are not as sharply defined as in the UZO, confirming earlier results of mock surveys extracted from unconstrained simulations (Schmalzing & Diaferio 2000). This disagreement

amplifies substantially when we consider the properties and the large-scale distribution of groups.

The group-finder algorithm strongly depends on the galaxy luminosity function. The numerical recipes adopted to form and evolve galaxies in the simulations provide a galaxy luminosity function which is considerably different from that of the UZC. We test that this difference is the major responsible for the model inability at reproducing the group properties. We assign new luminosities to the simulated galaxies according to the luminosity function of the UZC, while preserving the luminosity rank predicted by the model. We thus have new mock catalogues where galaxy luminosities distribute according to the UZC luminosity function (UZCLF), besides the catalogues where galaxy luminosities distribute according to the semi-analytic luminosity function (SALF).

Unlike the groups extracted from the SALF and the τ CDM-UZCLF mock catalogues, the groups extracted from the Λ CDM-UZCLF catalogue have statistical properties in satisfactory agreement with observations: group abundances by luminosity, harmonic radius, velocity dispersion and mass are generally within $3\text{-}\sigma$ errors, or less, from the UZC group abundances. These groups also reproduce the UZC relations between the group mass-to-light ratio and mass, and the galaxy number and mass, namely the halo occupation number. Finally, the Λ CDM-UZCLF groups, similarly to the UZC groups and unlike the SALF groups, show a weak correlation between the luminosity difference between the two brightest galaxies in a group and the total group luminosity. This result indicates that the two semi-analytic prescriptions of allowing merging of satellite galaxies only with the central galaxy of the dark matter halo and gas cooling only onto this same central galaxy produces a too large luminosity difference between the two brightest galaxies in a group.

The success in the statistical properties of groups, obtained by adopting the observed luminosity function, is not shared by the large-scale distribution of groups. Specifically, the simulated groups in the North Galactic Cap of the Λ CDM-UZCLF catalogue trace the large-scale distribution of galaxies at significance levels as much as seven times smaller than those of the UZC. This is a consequence of the looser large-scale structures in the models: in fact, the redshift-space correlation function of galaxies is more than $3\text{-}\sigma$ below the observations on scales larger than $6h^{-1}$ Mpc (Figure 11; Mathis et al. 2002) and the number of groups is 25% smaller than in the UZC (Table 3).

We therefore conclude that (1) the semi-analytic recipes used in Mathis et al. (2002) have serious difficulties at distributing the luminosity among galaxies correctly; and (2) even the most successful Λ CDM model does not yield cosmic structures as coherent as observed. Whereas the first problem might be solved, in principle, with more sophisticated semi-analytic modellings (e.g. Croton et al. 2006; Weinmann et al. 2006b) the second problem appears to be more fundamental, although the disagreement with observation is less dramatic: in this case, both different dark matter models and an appropriate treatment of the interplay between gas dynamics and dark matter might be necessary to reconcile the model with group properties.

ACKNOWLEDGMENTS

Part of this work served as the undergraduate thesis of LC at the University of Torino. AD acknowledges the hospitality of Chris Flynn and the Tuorla Astronomical Observatory where part of this work was carried out. We thank an anonymous referee for a prompt report and relevant comments, and Hughes Mathis and his collaborators for making publicly available their simulations. The simulations were carried out on the T3E supercomputer at the Computing Centre of the Max-Planck Society in Garching, Germany. The data are available at www.mpa-garching.mpg.de/galform/cr/data.shtml.

REFERENCES

- Abazajian K., et al., 2005, *ApJ*, 625, 613
 Allington-Smith J. R., Ellis R., Zirbel E. L., Oemler A. Jr., 1993, *ApJ* 404, 521
 Balogh M., et al., 2004, *MNRAS*, 348, 1355
 Barton E. J., Geller M. J., Kenyon S. J., 2003, *ApJ*, 582, 668
 Benson A. J., Cole S., Frenk C. S., Baugh C. M., Lacey C. G., 2000, *MNRAS*, 311, 793
 Berlind A. A., et al., 2003, *ApJ*, 593, 1
 Berlind A. A., et al., 2006, preprint (astro-ph/0601346)
 Berrier J. C., Bullock J. S., Barton E. J., Guenther H. D., Zentner A. R., Wechsler R. H., 2006, preprint (astro-ph/0604506)
 Bothun G. D., Cornell M. E., 1990, *AJ*, 99, 1004
 Brough S., Forbes D., Kilborn V., Couch W., 2006, preprint (astro-ph/0605279)
 Ceccarelli M. L., Valotto C., Lambas D. G., Padilla N., Giovanelli R., Haynes M., 2005, *ApJ*, 622, 853
 Croton D. J., et al., 2006, *MNRAS*, 365, 11
 Davis M., Huchra J. P., 1982, *ApJ*, 254, 437
 Diaferio A., Kauffmann G., Colberg J. M., White S. D. M., 1999, *MNRAS*, 307, 537
 Eke V. R., et al., 2004a, *MNRAS*, 348, 866
 Eke V. R., et al., 2004b, *MNRAS*, 355, 769
 Eke V. R., Baugh C. M., Cole S., Frenk C. S., Navarro J. F., 2006, preprint (astro-ph/0510643)
 Ellingson E., 2004, in *Outskirts of Galaxy Clusters: Intense Life in the Suburbs*, Proceedings of the IAU Coll. 195, Torino, ed. by A. Diaferio, Cambridge University Press, p. 327
 Falco E. E. et al., 1999, *PASP*, 111, 438
 Fisher K. B., Davis M., Strauss M. A., Yahil A., Huchra J. P., 1994, *MNRAS*, 267, 927
 Fisher K. B., Huchra J. P., Strauss M. A., Davis M., Yahil A., Schlegel D., 1995, *ApJS*, 100, 69
 Focardi P., Kelm B., 2002, *A&A*, 391, 35
 Focardi P., Zitelli V., Marinoni S., Kelm B., 2006, *A&A*, preprint (astro-ph/0605152)
 Frederic J. J., 1995a, *ApJS*, 97, 259
 Frederic J. J., 1995b, *ApJS*, 97, 275
 Ganon G., Hoffman Y., 1993, *ApJ*, 415, L5
 Girardi M., Boschini W., da Costa L.N., 2000, *A&A*, 353, 57
 Girardi M., Mardirossian F., Marinoni C., Mezzetti M., Rigoni E., 2003, *A&A*, 410, 461

- Giuricin G., Samurović S., Girardi M., Mezzetti M., Marini C., 2001, *ApJ*, 554, 857
- Hickson P., 1997, *ARA&A*, 35, 357
- Hoffman Y., Ribak E., 1991, *ApJ*, 380, L5
- Hoffman Y., Ribak E., 1992, *ApJ*, 396, 448
- Hoyle F., Vogeley M. S., 2002, *ApJ*, 566, 641
- Huchra J. P., 1976, *AJ*, 81, 951
- Jarrett T. H., 2000, *PASP*, 112, 1008
- Jing Y., Zhang J., 1988, *A&A*, 190, 21
- Jing Y. P., Mo H. J., Börner G., 1998, *ApJ*, 494, 1
- Kauffmann G., Nusser A., Steinmetz M., 1997, *MNRAS*, 286, 795
- Kauffmann G., Colberg J. M., Diaferio A., White S. D. M., 1999, *MNRAS*, 303, 188
- Kelm B., Focardi P., 2004, *A&A*, 418, 937
- Kodama T., Smail I., Nakata F., Okamura S., Bower R. G., 2001, *ApJ*, 562, L9
- Kochanek C. S., White M., Huchra J., Macri L., Jarrett T. H., Schneider S. E., Mader J., 2003, *ApJ*, 585, 161
- Kravtsov A. V., Berlind A. A., Wechsler R. H., Klypin A. A., Gottlöber S., Allgood B., Primack J. R., 2004, *ApJ*, 609, 35
- Lanzoni B., Ciotti L., Cappi A., Tormen G., Zamorani G., 2004, *ApJ*, 600, 640
- Lee B. C., et al., 2004, *AJ*, 127, 1811
- Lin Y.-T., Mohr J. J., Stanford S. A., 2004, *ApJ*, 610, 745
- Magliocchetti M., Porciani C., 2003, *MNRAS*, 346, 186
- Mahdavi A., Böhringer H., Geller M. J., Ramella M., 2000, *ApJ*, 534, 114
- Marinoni M., Hudson M. J., 2002, *ApJ*, 569, 101
- Martínez H. J., Muriel H., 2006, *MNRAS*, in press
- Marzke R. O., Huchra J. P., Geller M. J., 1994, *ApJ*, 428, 43
- Mathis H., Lemson G., Springel V., Kauffmann G., White S. D. M., Eldar A., Dekel A., 2002, *MNRAS*, 333, 739
- Martínez H. J., Zandivarez A., Domínguez M., Merchán M. E., Lambas D. G., 2002a, *MNRAS*, 333, L31
- Martínez H. J., Zandivarez A., Merchán M. E., Domínguez M. J. L., 2002b, *MNRAS*, 337, 1441
- Mendes de Oliveira C., Amram P., Plana H., Balkowski C., 2003, *AJ*, 126, 2635
- Moore B., Frenk C. S., White S. D. M., 1993, *MNRAS*, 261, 827
- Nolthenius R., White S. D. M., 1987, *MNRAS*, 235, 505
- Padilla N. D., Merchán M. E., Valotto C. A., Lambas D. G., Maia M. A. G., 2001, *ApJ*, 554, 873
- Padilla N. D., et al., 2004, *MNRAS*, 352, 211
- Padmanabhan N., Tegmark M., Hamilton A. J. S., 2001, *ApJ*, 550, 52
- Pisani A., Ramella M., Geller M. J., 2003, *AJ*, 126, 1677
- Plionis M., Basilakos S., Tovmassian H., 2004, *MNRAS*, 352, 1323
- Popesso P., Biviano A., Böhringer H., Romaniello M., 2006, preprint (astro-ph/0606260)
- Postman M., Geller M. J., 1984, *ApJ*, 281, 95
- Ramella M., Geller M. J., Huchra J. P., 1990, 353, 51
- Ramella M., Pisani A., Geller M. J., 1997, *AJ*, 113, 483
- Ramella M., et al., 1999, *A&A*, 342, 1
- Ramella M., Geller M. J., Pisani A., da Costa L. N., 2002, *AJ*, 123, 2976
- Rines K., Geller M. J., Diaferio A., Kurtz M. J., Jarrett T. H., 2004, *AJ*, 128, 1078
- Roukema B. F., Quinn P. J., Peterson B. A., Rocca-Volmerange B., 1997, *MNRAS* 292, 835
- Schmalzing J., Diaferio A., 2000, *MNRAS*, 312, 638
- Scoccimarro R., Sheth R. K., Hui L., Jain B., 2001, *ApJ*, 546, 20
- Sheth R. K., 2005, *MNRAS*, 364, 796
- Sheth R. K., Jimenez R., Panter B., Heavens A., 2006, preprint (astro-ph/0604581)
- Skibba R., Sheth R. K., Connolly A. J., Scranton R., 2006, *MNRAS*, 369, 68
- Springel V., Yoshida N., White S. D. M., 2001, *New Astronomy*, 6, 79
- Tanaka M., Kodama T., Arimoto N., Okamura S., Umetsu K., Shimasaku K., Tanaka I., Yamada T., 2005, *MNRAS*, 362, 268 (Erratum: 2006, *MNRAS*, 366, 1551)
- Tanvuia L., Kelm B., Focardi P., Rampazzo R., Zeilinger W. W., 2003, *AJ*, 126, 1245
- Tinker J. L., Weinberg D. H., Zheng Z., Zehavi I., 2005, *ApJ*, 631, 41
- Tovmassian H., Plionis M., Torres-Papaqui J. P., 2006, preprint (astro-ph/0605144)
- Tran K.-V. H., Simard L., Zabludoff A. I., Mulchaey J. S., 2001, *ApJ*, 549, 172
- Trasarti-Battistoni R., Invernizzi G., Bonometto S.A., 1997, *ApJ*, 475, 1
- van den Bosch F. C., Yang X., Mo H. J., 2003a, *MNRAS*, 340, 771 (see also erratum astro-ph/0210495)
- van den Bosch F. C., Mo H. J., Yang X., 2003b, *MNRAS*, 345, 923 (see also erratum astro-ph/0301104)
- Verheijen M. A. W., 2004, in *Outskirts of Galaxy Clusters: Intense Life in the Suburbs*, Proceedings of the IAU Coll. 195, Torino, ed. by A. Diaferio, Cambridge University Press, p. 394
- Weinmann S. M., van den Bosch F. C., Yang X., Mo H. J., 2006a, *MNRAS*, 366, 2
- Weinmann S. M., van den Bosch F. C., Yang X., Mo H. J., Croton D. J., Moore B., 2006b, preprint (astro-ph/0606458)
- Yang X., Mo H. J., Jing Y. P., van den Bosch F. C., 2005a, *MNRAS*, 358, 217
- Yang X., Mo H. J., van den Bosch F. C., Jing Y. P., 2005b, *MNRAS*, 356, 1293
- Zandivarez A., Merchán M. E., Padilla N. D. 2003, *MNRAS* 344, 247
- Zandivarez A., Martínez H. J., Merchán M. E., 2006, preprint (astro-ph/0602405)
- Zehavi I., et al., 2005, *ApJ*, 630, 1
- Zheng Z., et al., 2005, *ApJ*, 633, 791